Electronic Supplementary Material (ESI) for New Journal of Chemistry.

Solvatochromism and fluorescence response of a halogen bonding anion receptor

J. Sun, A. M. Riel, and O. B. Berryman*

Department of Chemistry and Biochemistry, University of Montana, 32 Campus Dr, Missoula MT, 59812, USA
*orion.berryman@umontana.edu

Contents

A. General methods

All reagents were obtained from commercial sources and were used without further purification unless otherwise noted. All the solvents used for UV-Vis and fluorescence studies were spectrophotometric grade (99.7+%). All UV-Vis spectra were collected on a Cary 60 spectrometer at 298 K. All fluorescence spectra were collected on a Cary Eclipse spectrometer at 298 K. All spectra were collected using a quartz cell fitted with a Teflon stopper, with a path length of 10.0 mm. In all cases, 0.02mM was chosen as the working concentration for each receptor such that the peak absorbance value was approximately 0.2 to 0.5. Measurements were carried out using Hamilton gastight syringes and titrations were carried out using Hamilton microliter syringes. After each addition, the cell was stoppered and shook for two minutes to ensure complete mixing.

In order to keep the concentration of the receptor (host) constant throughout the titration, the receptor solution was used to prepare the anion (guest) solution. UV-Vis titrations were carried out by adding aliquots of the anion (guest) solution to a known volume of receptor (host) solution.

B. Solvatochromism of neutral receptors 1a and 1b

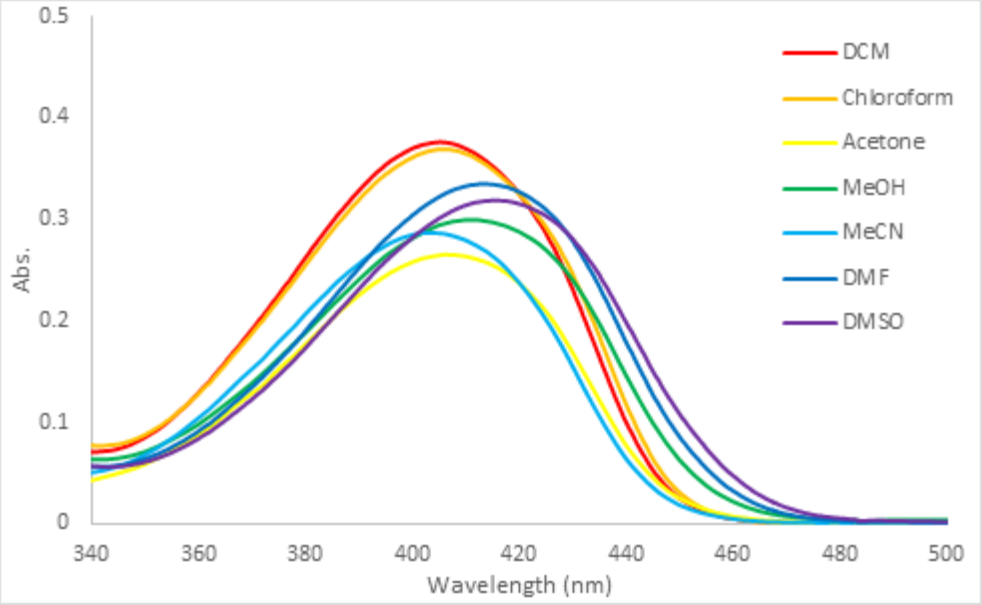

Figure S1. UV-Vis absorption spectrum of **1a** in various solvents.

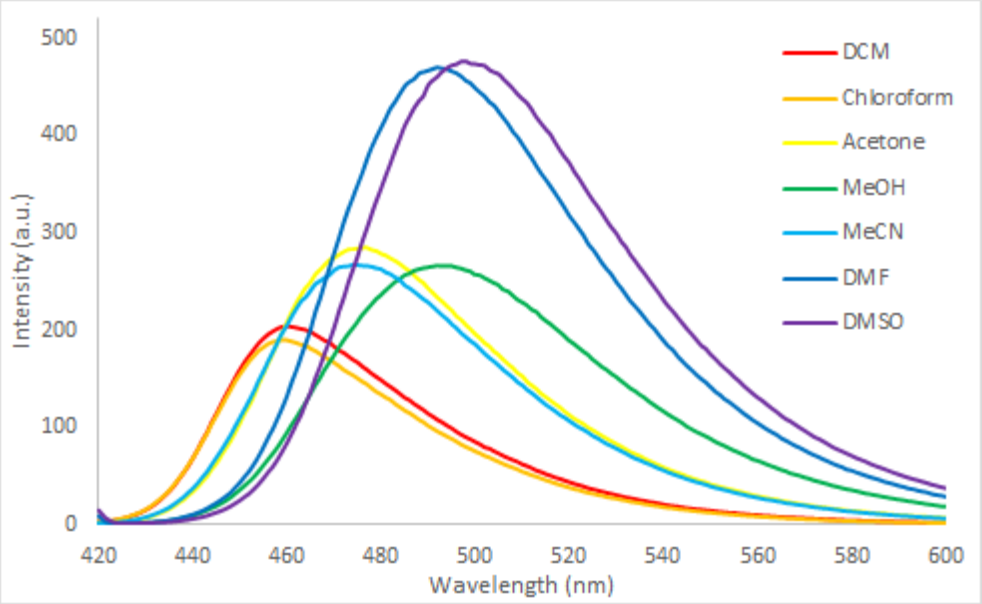

Figure S2. Fluorescence emission spectrum of **1a** in various solvents. Slit (excitation/emission) = 5 nm. $\lambda_{ex\ DCM}$= 405 nm, $\lambda_{ex\ Chloroform}$= 406 nm, $\lambda_{ex\ Acetone}$= 406 nm, $\lambda_{ex\ methanol}$= 411 nm, $\lambda_{ex\ MeCN}$= 405 nm, $\lambda_{ex\ DMF}$= 413.5 nm, $\lambda_{ex\ DMSO}$= 415.5 nm.

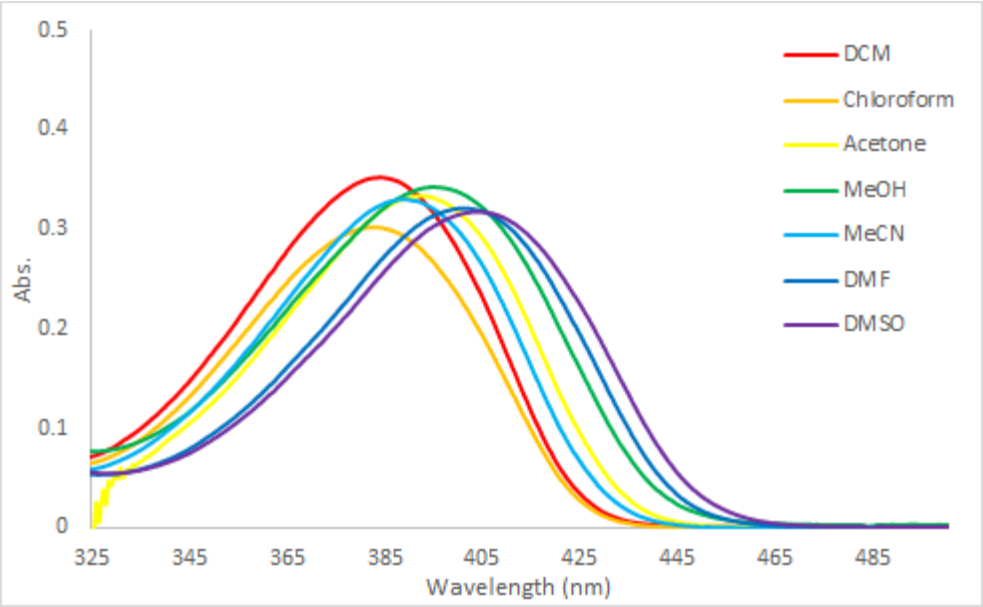

Figure S3. UV-Vis absorption spectrum of **1b** in various solvents.

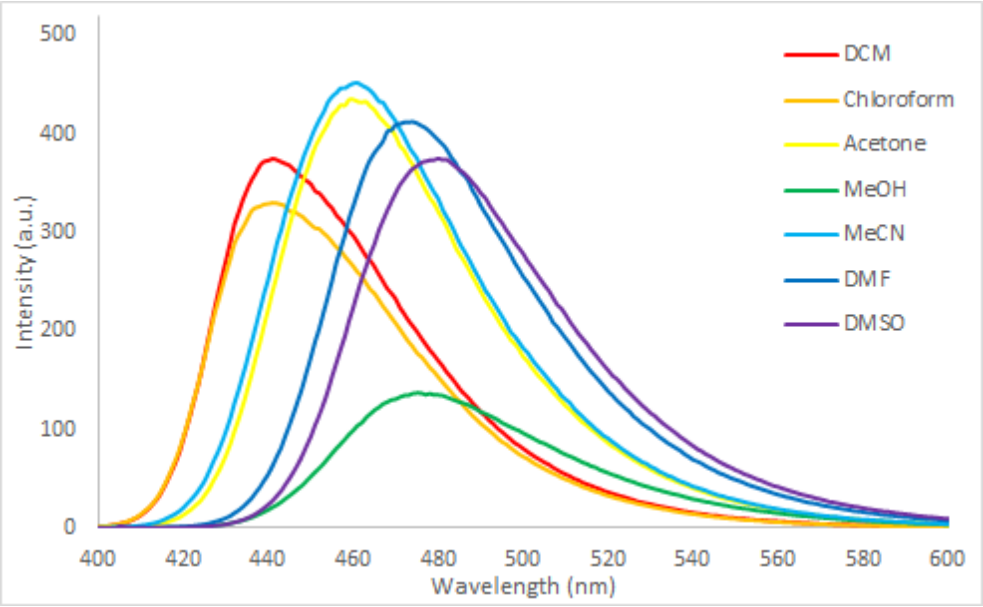

Figure S4. Fluorescence emission spectrum of **1b** in various solvents. Slit (excitation/emission) = 2.5 nm. $\lambda_{ex\ DCM}$= 384.5 nm, $\lambda_{ex\ Chloroform}$= 382 nm, $\lambda_{ex\ Acetone}$= 392.5 nm, $\lambda_{ex\ methanol}$= 395 nm, $\lambda_{ex\ MeCN}$ = 388 nm, $\lambda_{ex\ DMF}$= 401.5 nm, $\lambda_{ex\ DMSO}$= 404 nm.

C. Solvatochromism of charged receptors 2a and 2b

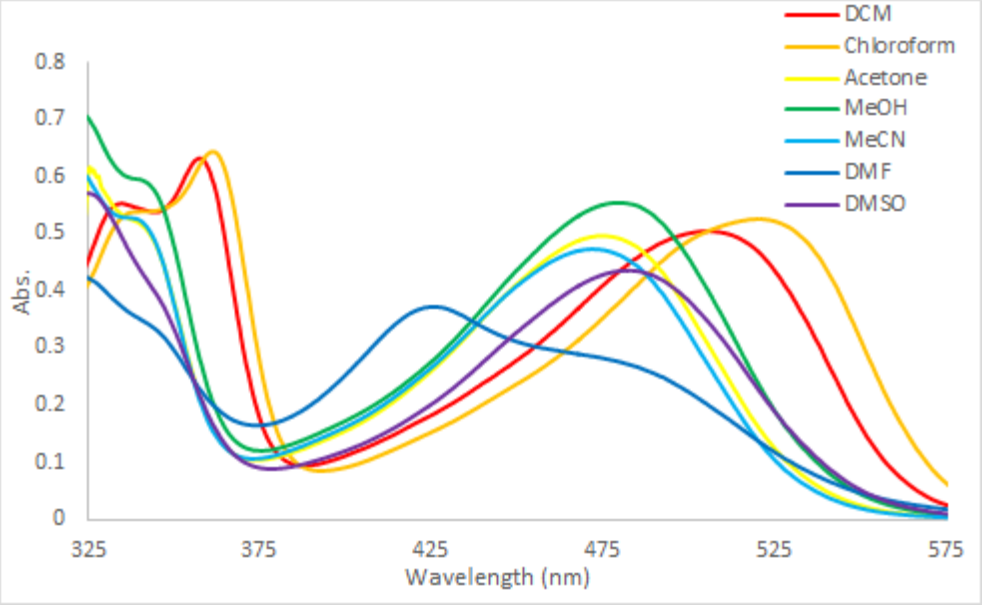

Figure S5. UV-Vis absorption spectrum of **2a** in various solvents.

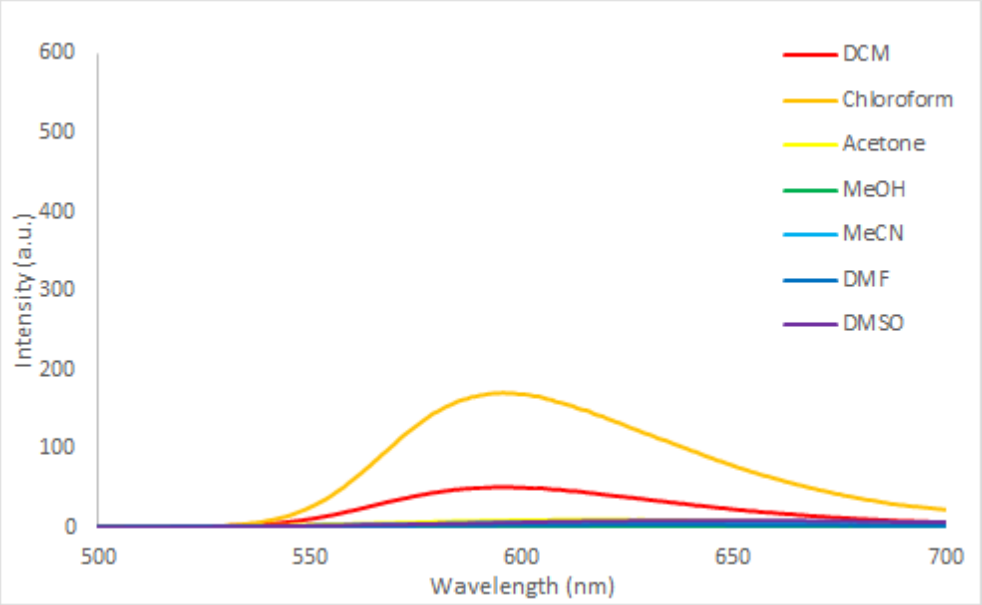

Figure S6. Fluorescence emission spectrum of **2a** in various solvents. Slit (excitation/emission) = 5 nm. $\lambda_{ex\ DCM}$= 505.5 nm, $\lambda_{ex\ Chloroform}$= 521 nm, $\lambda_{ex\ Acetone}$= 475 nm, $\lambda_{ex\ methanol}$= 479 nm, $\lambda_{ex\ MeCN}$ = 472 nm, $\lambda_{ex\ DMF}$= 425.5 nm, $\lambda_{ex\ DMSO}$= 482.5 nm.

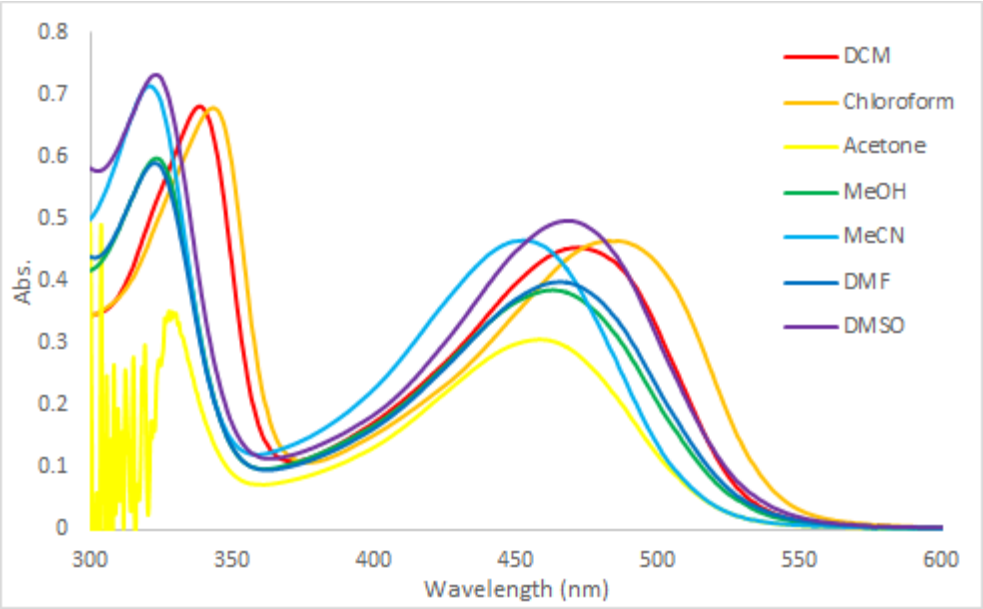

Figure S7. UV-Vis absorption spectrum of **2b** in various solvents.

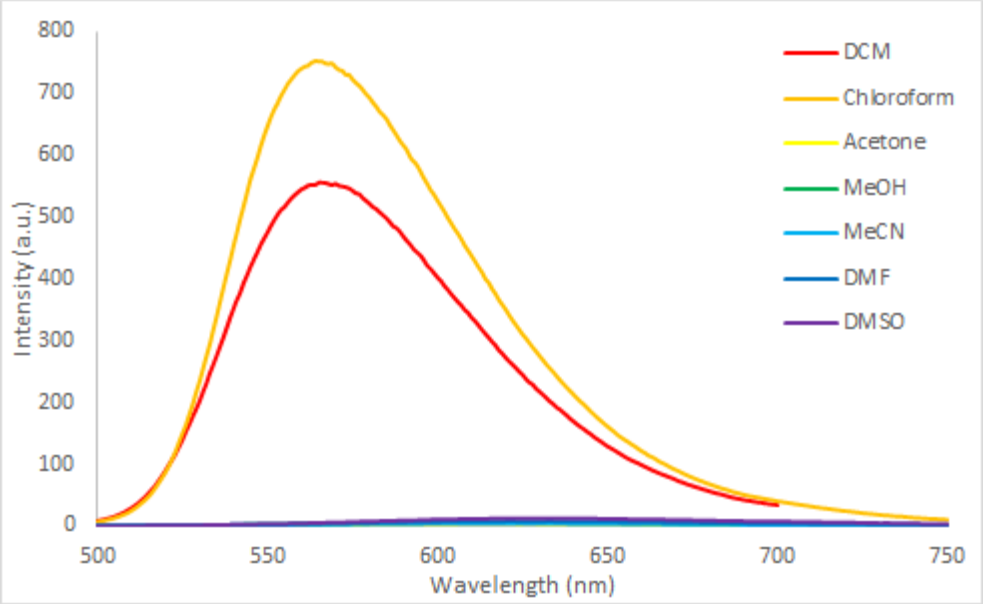

Figure S8. Fluorescence emission spectrum of **2b** in various solvents. Slit (excitation/emission) = 5 nm. $\lambda_{ex\ DCM}$= 472 nm, $\lambda_{ex\ Chloroform}$= 482.5 nm, $\lambda_{ex\ Acetone}$= 458.5 nm, $\lambda_{ex\ methanol}$= 463.5 nm, $\lambda_{ex\ MeCN}$ = 453.5 nm, $\lambda_{ex\ DMF}$= 465.5 nm, $\lambda_{ex\ DMSO}$= 468 nm.

D. Linear free energy relationships

Linear correlations between $1/\lambda_{max}$ of UV-Vis spectra and solvent polarity were conducted for neutral receptors **1a**,**b** and charged receptors **2a**,**b** using four solvent polarity parameters (dielectric constant, dipole moment, $E_T(30)$[1] and π*scale[2]), respectively.

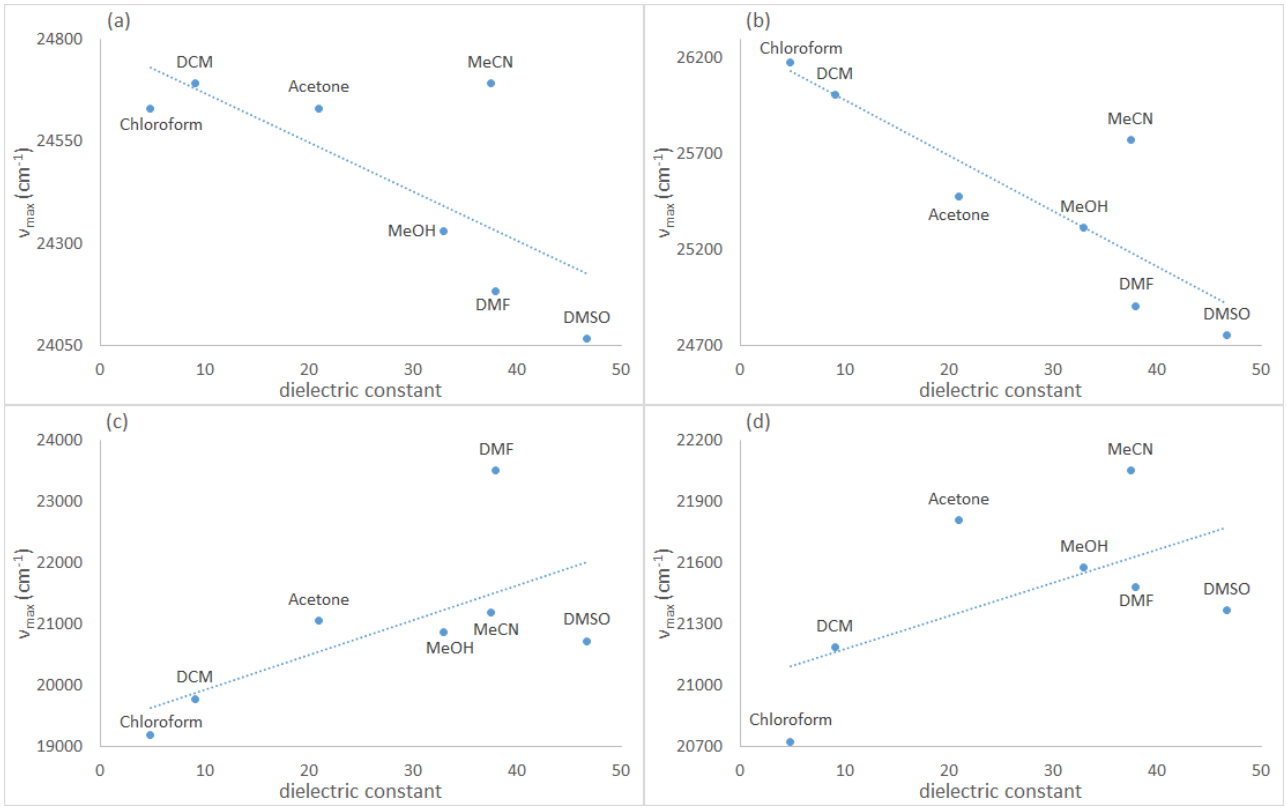

Figure S9. Linear correlation between ν_{max} and dielectric constant for neutral receptors **1a** (a), **1b** (b) and charged receptors **2a** (c), **2b** (d).

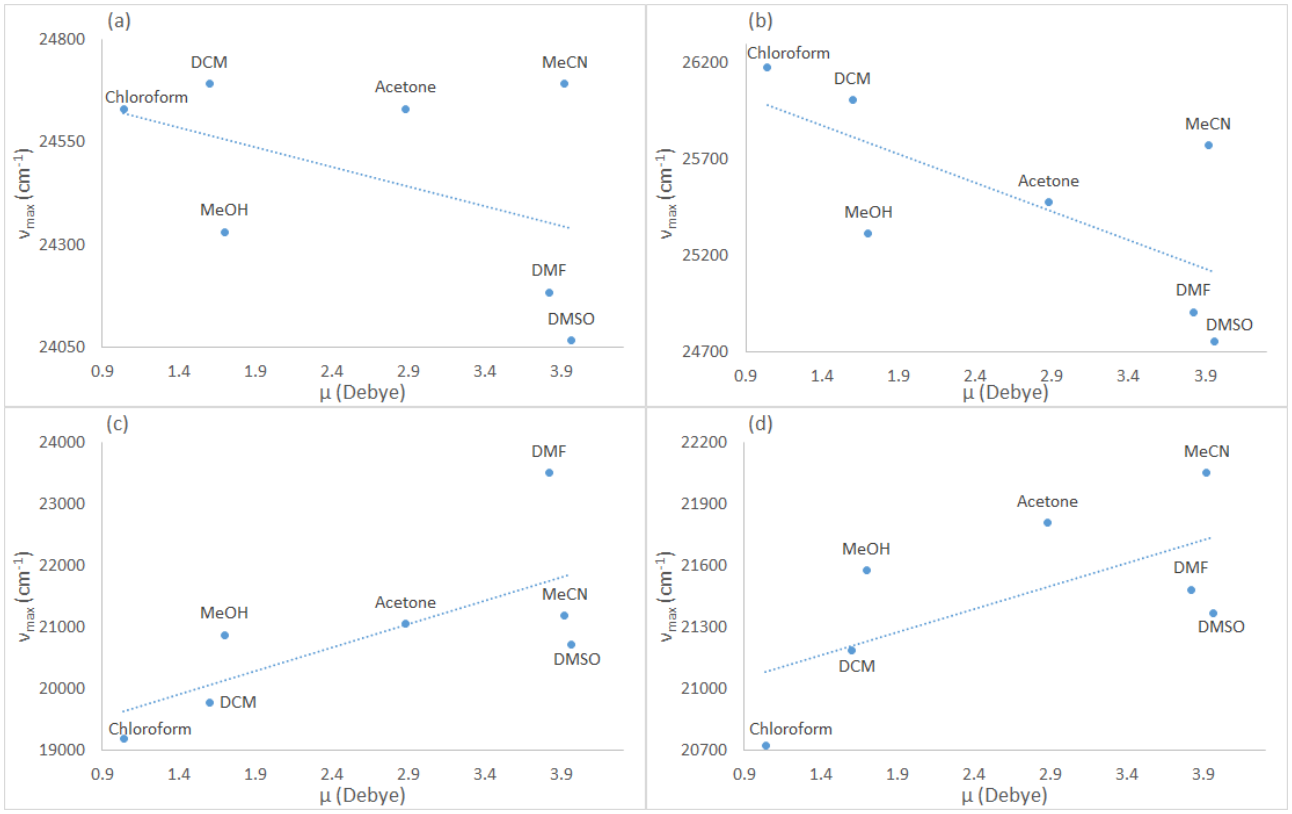

Figure S10. Linear correlation between ν_{max} and dipole moment for neutral receptors **1a** (a), **1b** (b) and charged receptors **2a** (c), **2b** (d).

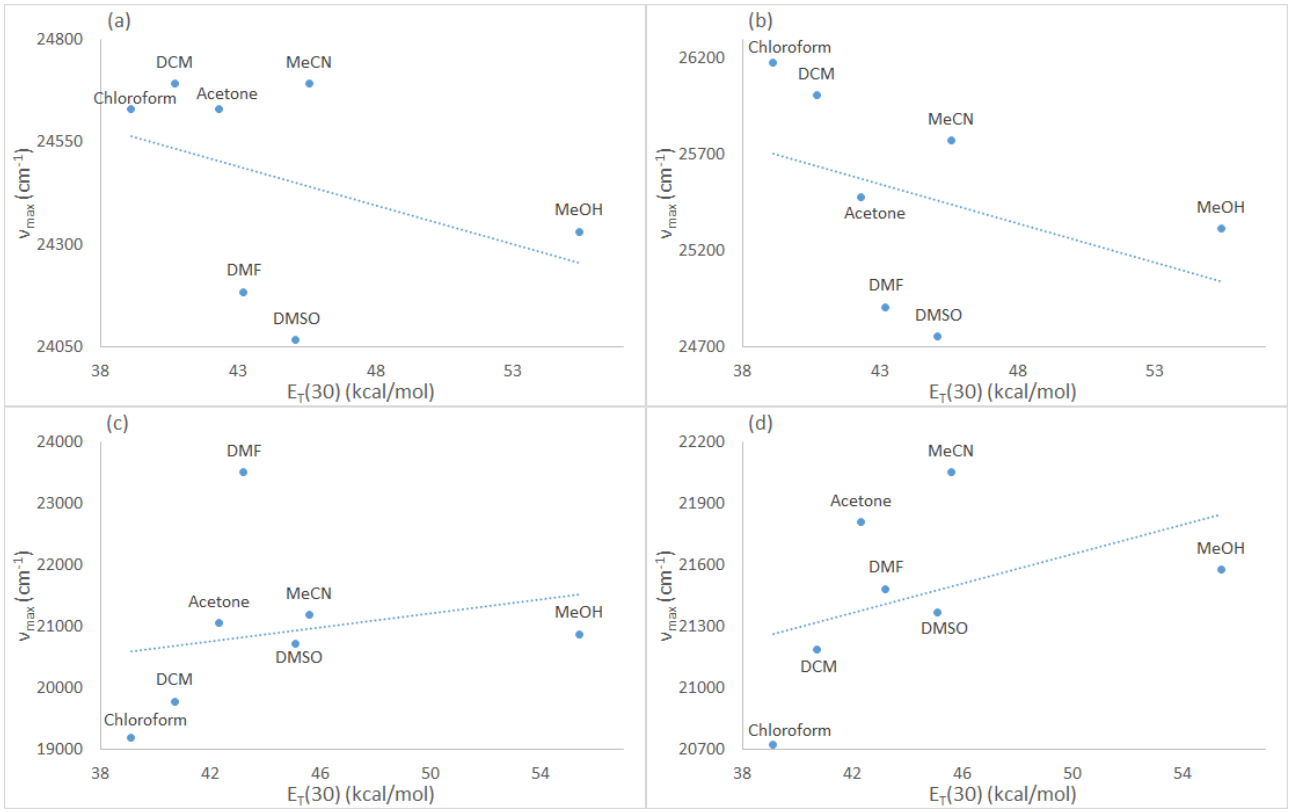

Figure S11. Linear correlation between ν_{max} and E_T(30) for neutral receptors **1a** (a), **1b** (b) and charged receptors **2a** (c), **2b** (d).

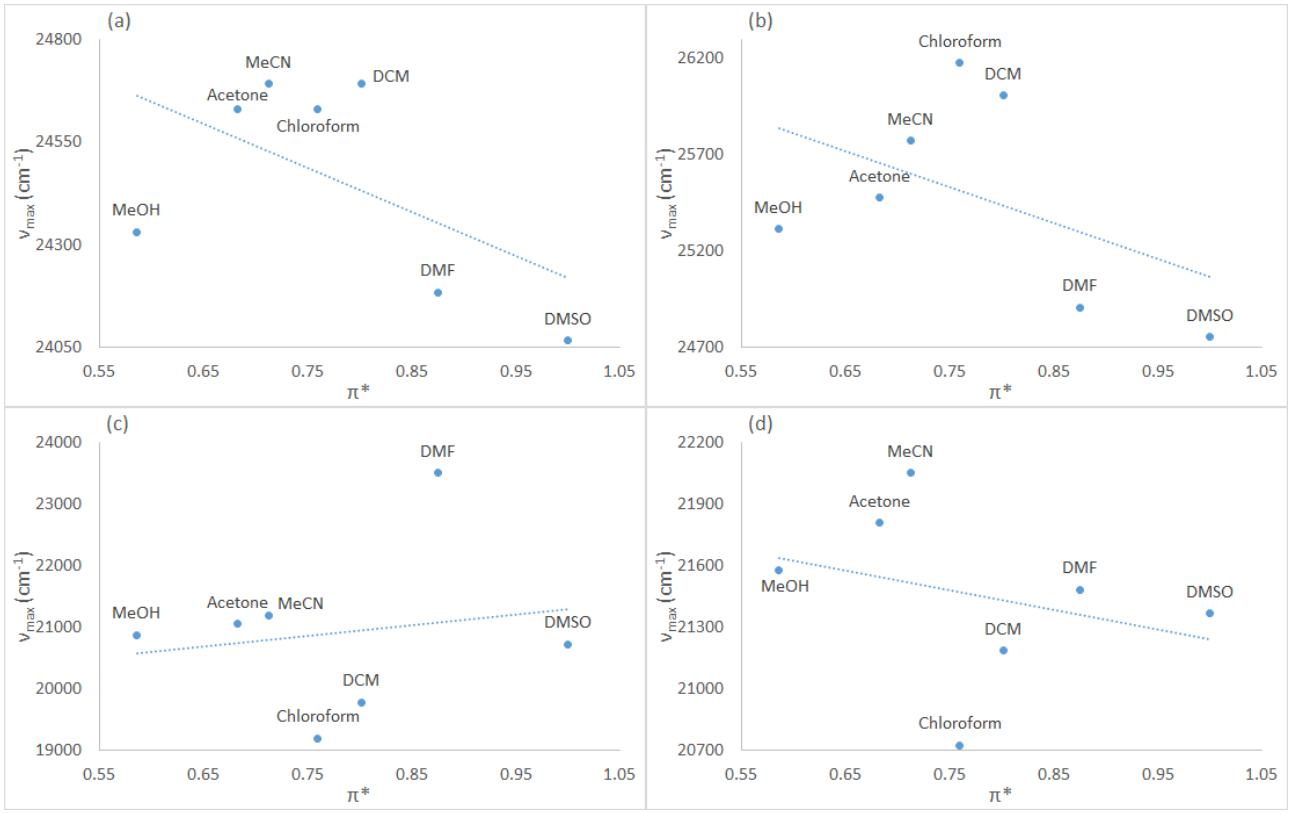

Figure S12. Linear correlation between ν_{max} and π* for neutral receptors **1a** (a), **1b** (b) and charged receptors **2a** (c), **2b** (d).

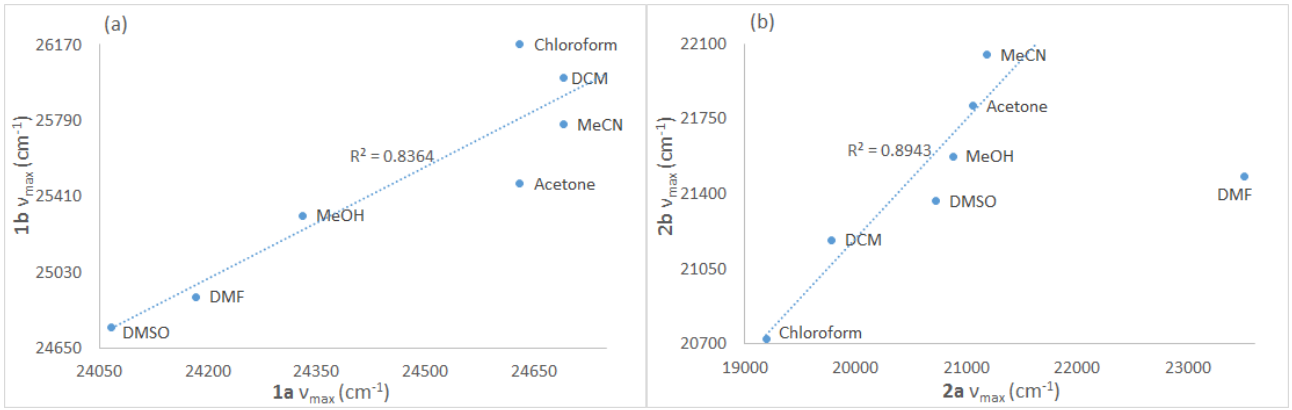

Figure S13. Linear correlation between (a) absorbance ν_{max} of neutral iodinated receptor **1a** and non-iodinated receptor **1b**, (b) absorbance ν_{max} of charged iodinated receptor **2a** and non-iodinated receptor **2b**.

E. Anion binding studies

All spectra were recorded at 20 µM of receptor in dichloromethane solution. Slit of excitation and emission for fluorescence experiment in this section is set up to 5 nm unless otherwise noted.

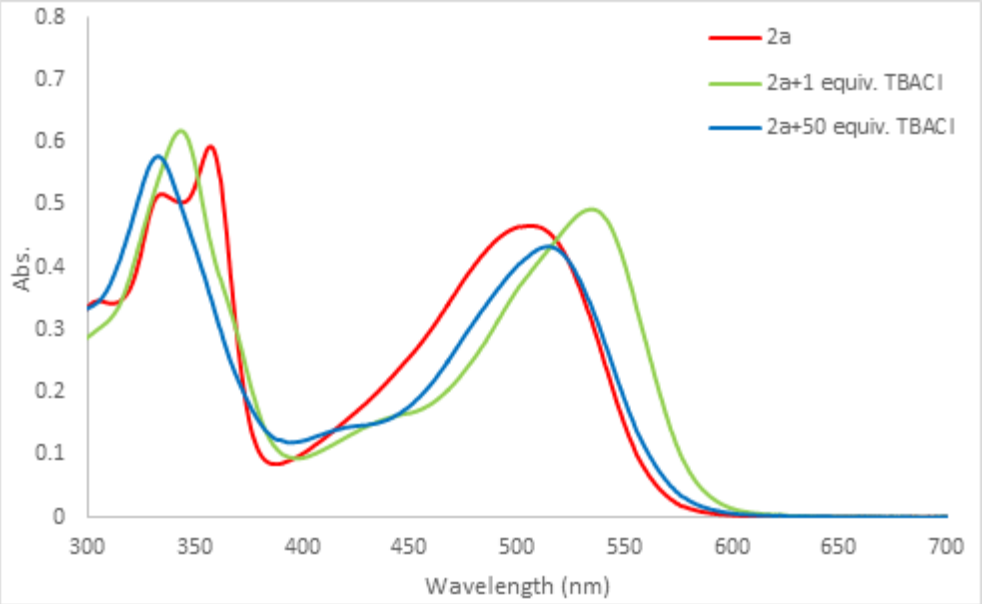

Figure S14. UV-Vis absorption spectrum of **2a** upon addition of TBA^+Cl^-.

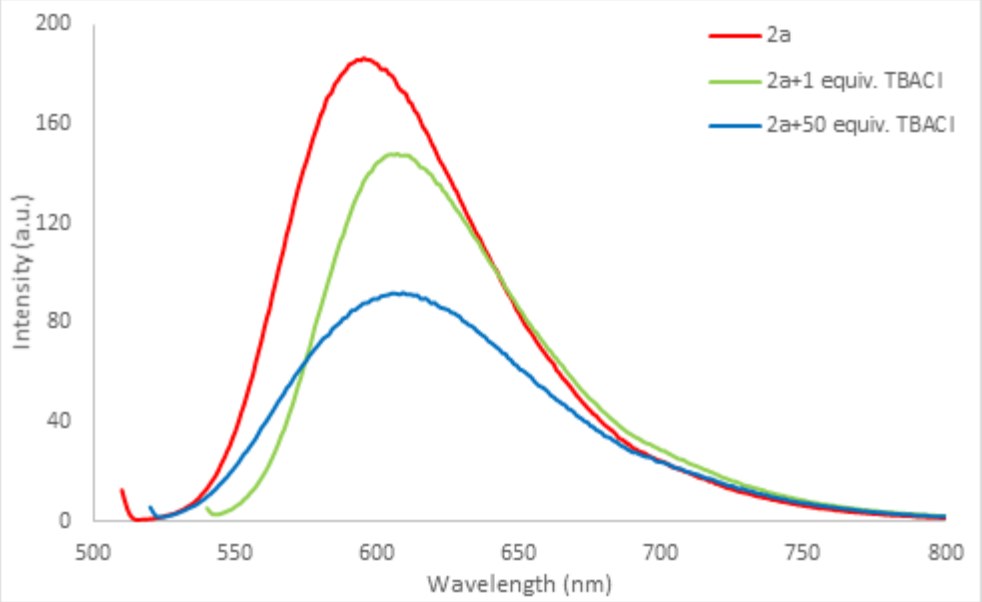

Figure S15. Fluorescence emission spectrum of **2a** upon addition of TBA^+Cl^-.
λ_{ex} red= 506.5 nm, λ_{ex} green= 534.5 nm, λ_{ex} blue= 514.5 nm.

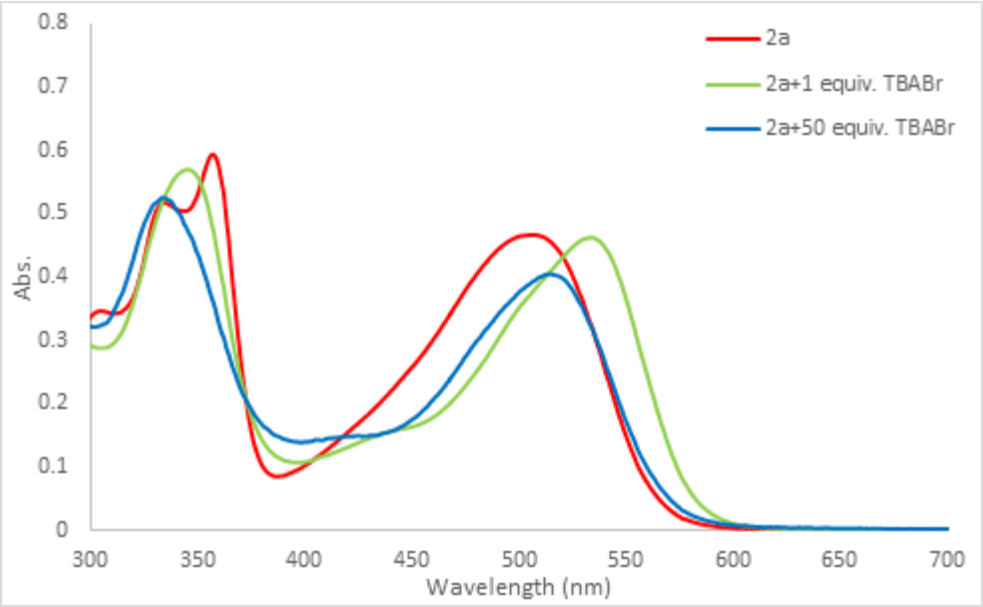

Figure S16. UV-Vis absorption spectrum of **2a** upon addition of $TBA^{+}Br^{-}$.

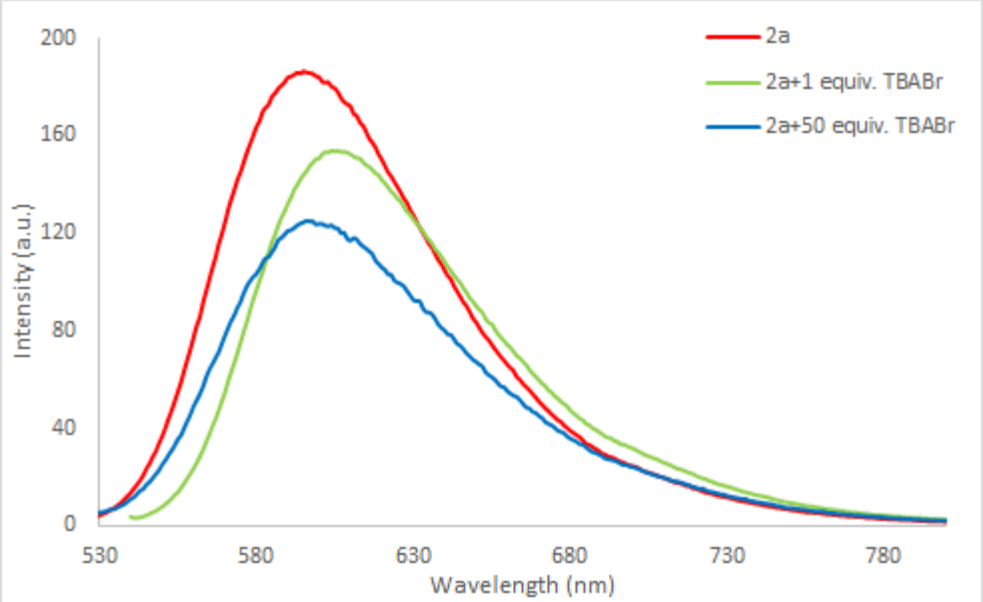

Figure S17. Fluorescence emission spectrum of **2a** upon addition of $TBA^{+}Br^{-}$.
λ_{ex} red= 506.5 nm, λ_{ex} green= 534 nm, λ_{ex} blue= 514.5 nm.

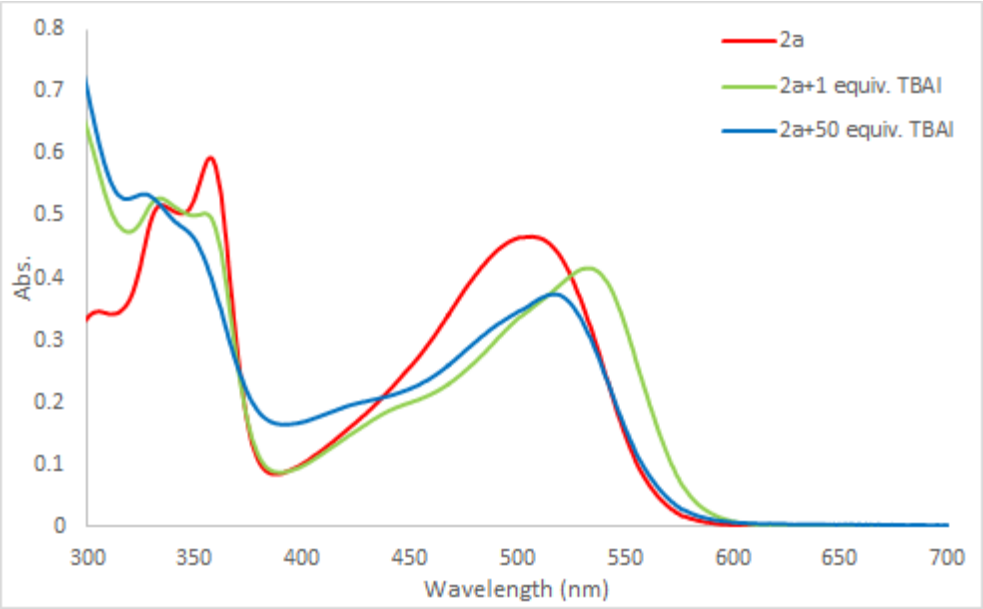

Figure S18. UV-Vis absorption spectrum of **2a** upon addition of $TBA^{+}I^{-}$.

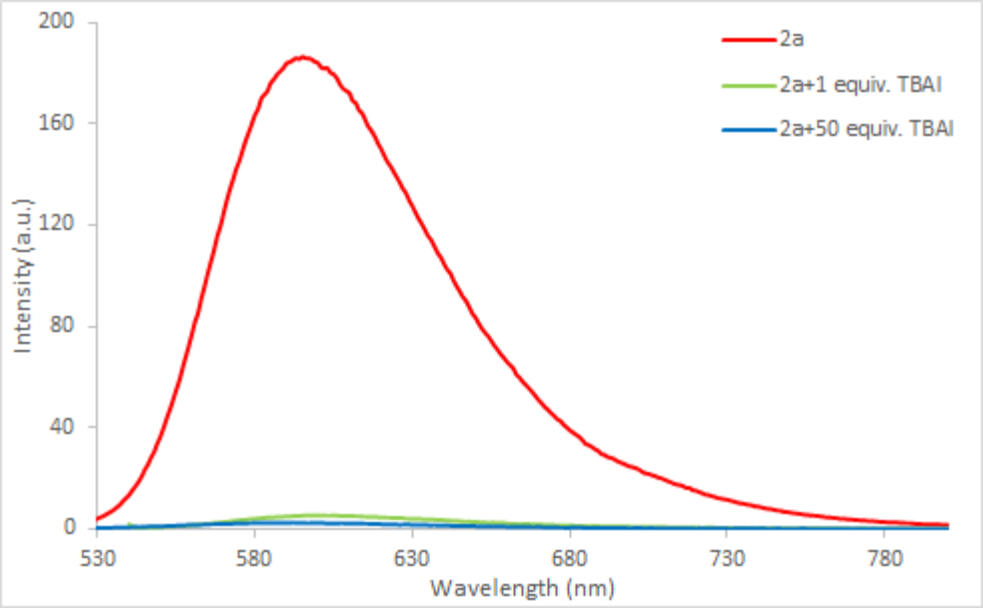

Figure S19. Fluorescence emission spectrum of **2a** upon addition of $TBA^{+}I^{-}$.
λ_{ex} red= 506.5 nm, λ_{ex} green= 534 nm, λ_{ex} blue= 517.5 nm.

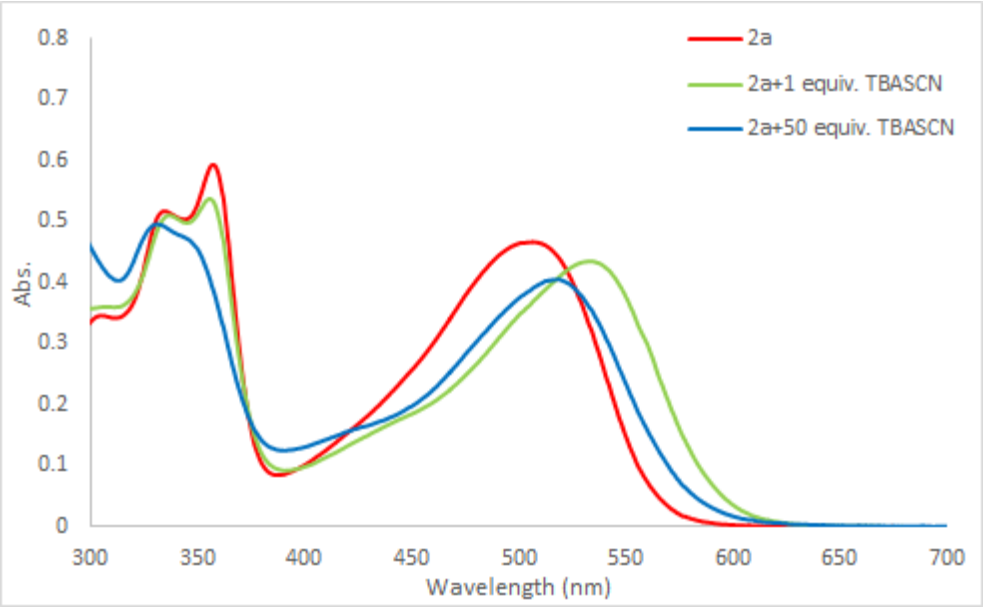

Figure S20. UV-Vis absorption spectrum of **2a** upon addition of $TBA^{+}SCN^{-}$.

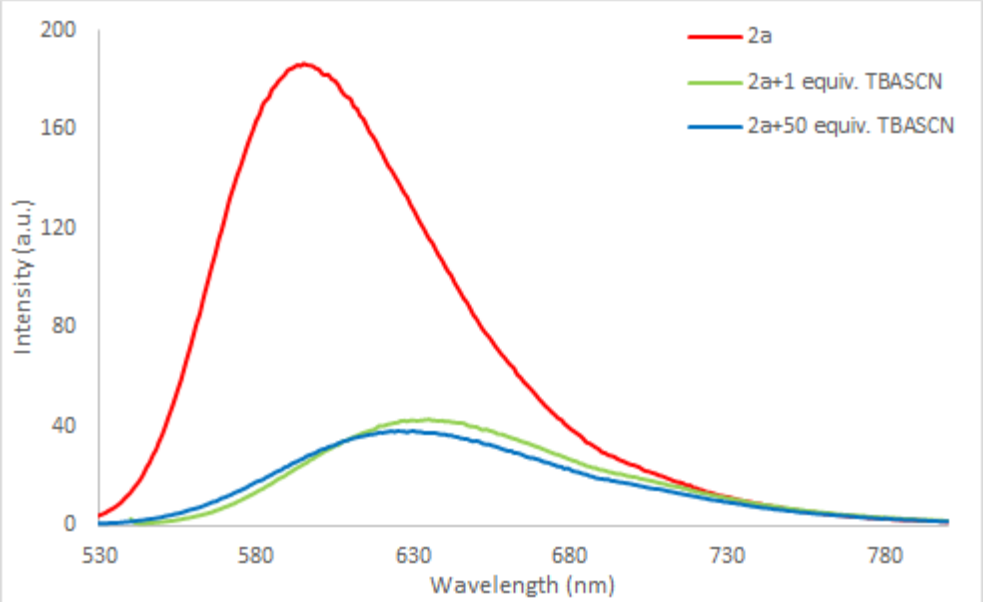

Figure S21. Fluorescence emission spectrum of **2a** upon addition of $TBA^{+}SCN^{-}$. λ_{ex} red= 506.5 nm, λ_{ex} green= 534 nm, λ_{ex} blue= 518.5 nm.

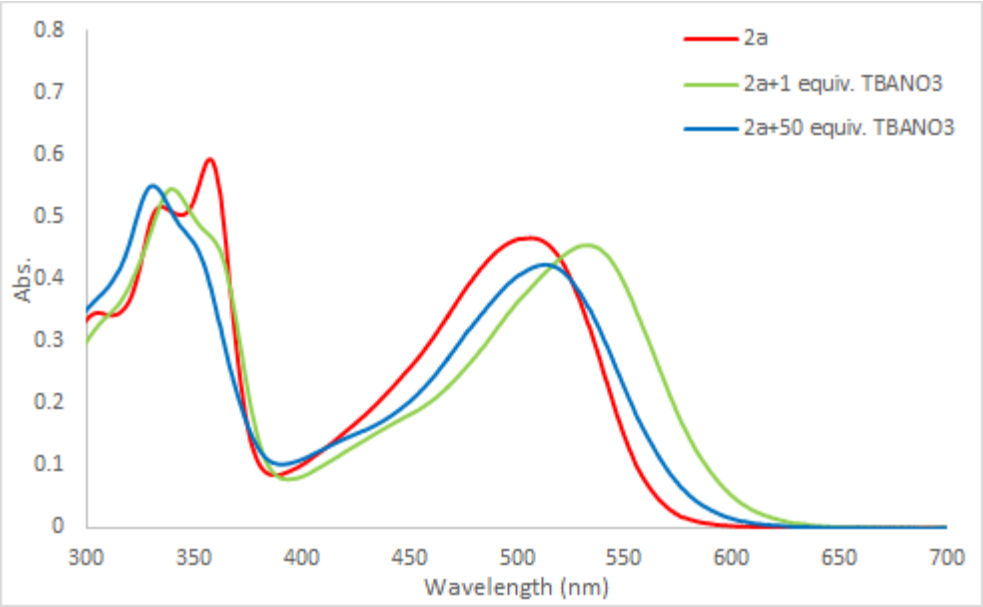

Figure S22. UV-Vis absorption spectrum of **2a** upon addition of $TBA^{+}NO_3^{-}$.

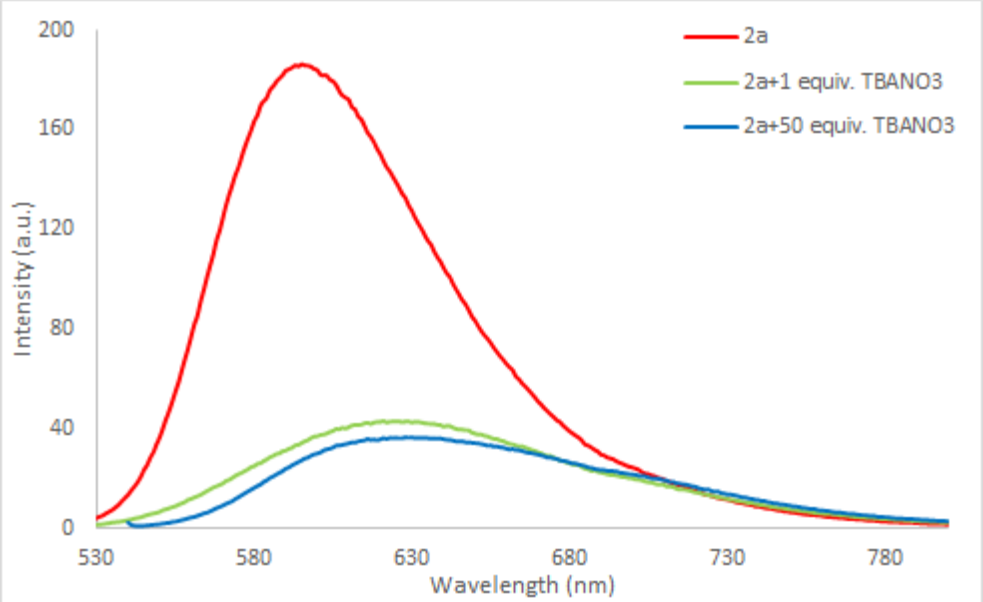

Figure S23. Fluorescence emission spectrum of **2a** upon addition of $TBA^{+}NO_3^{-}$. λ_{ex} red= 506.5 nm, λ_{ex} green= 534 nm, λ_{ex} blue= 513 nm.

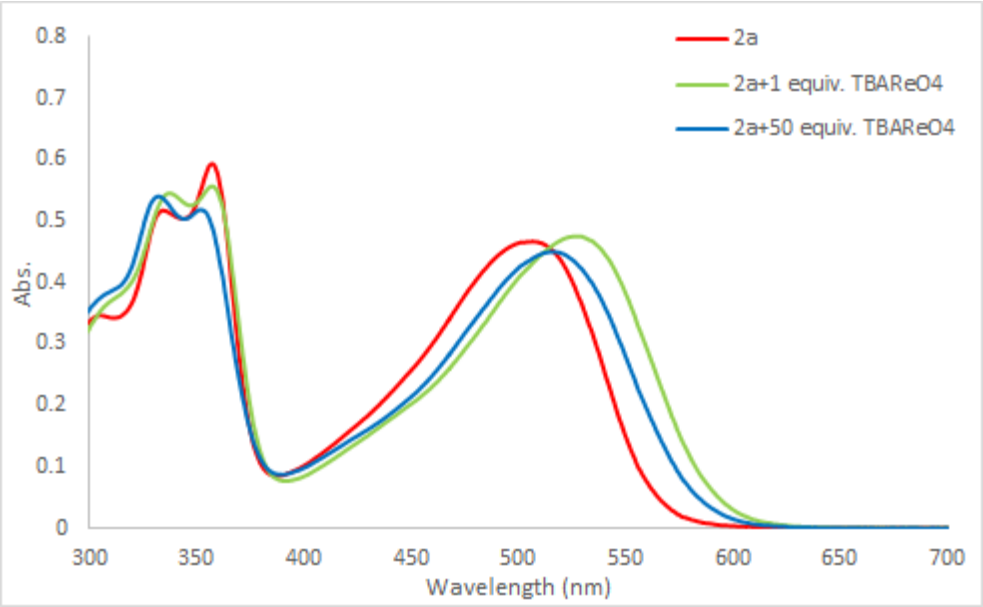

Figure S24. UV-Vis absorption spectrum of **2a** upon addition of $TBA^{+}ReO_4^{-}$.

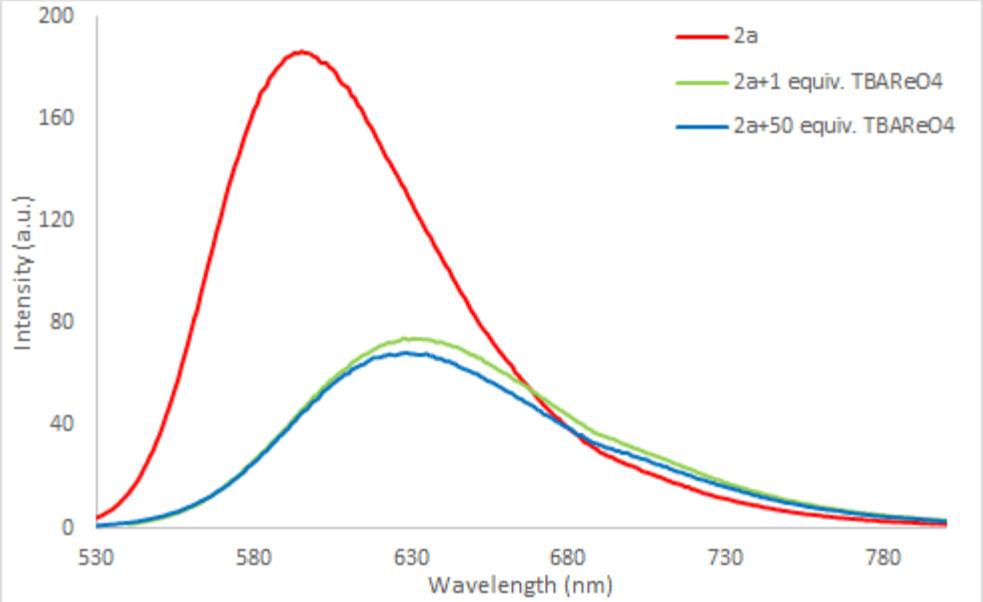

Figure S25. Fluorescence emission spectrum of **2a** upon addition of $TBA^{+}ReO_4^{-}$. λ_{ex} red= 506.5 nm, λ_{ex} green= 526.5 nm, λ_{ex} blue= 514.5 nm.

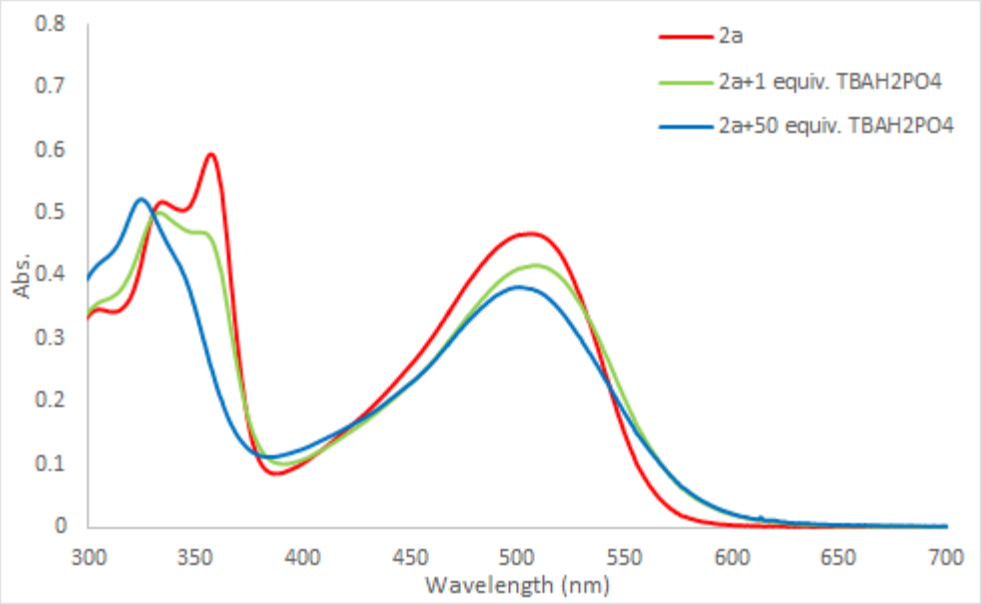

Figure S26. UV-Vis absorption spectrum of **2a** upon addition of $TBA^{+}H_2PO_4^{-}$.

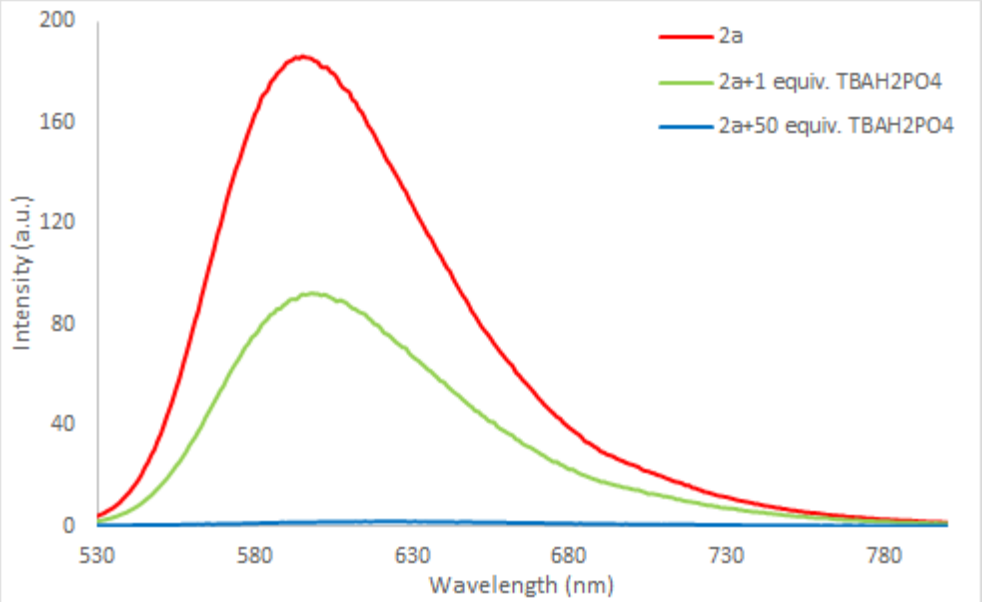

Figure S27. Fluorescence emission spectrum of **2a** upon addition of $TBA^{+}H_2PO_4^{-}$. λ_{ex} red= 506.5 nm, λ_{ex} green= 509 nm, λ_{ex} blue= 501 nm.

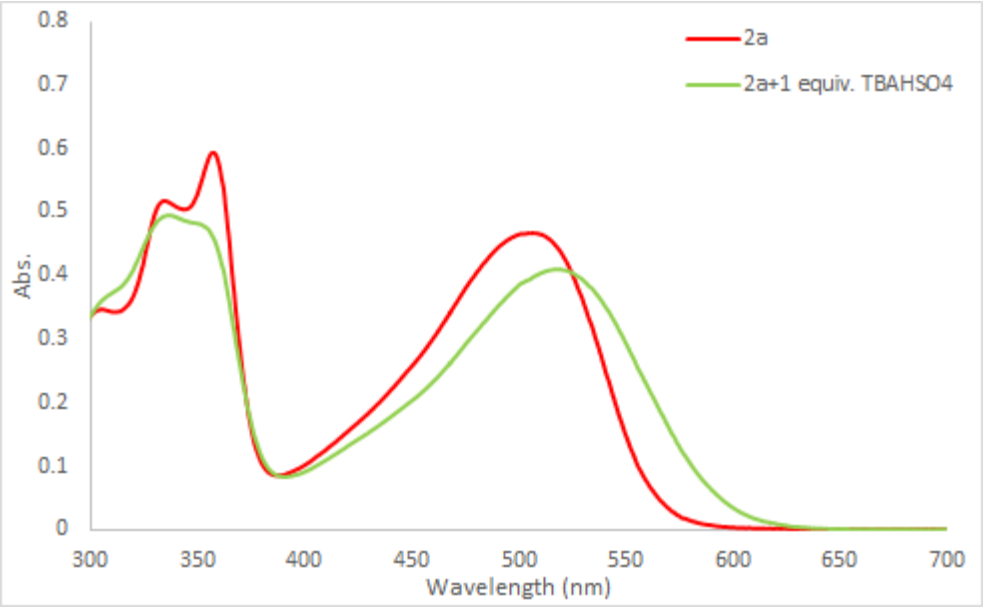

Figure S28. UV-Vis absorption spectrum of **2a** upon addition of $TBA^{+}HSO_4^{-}$.

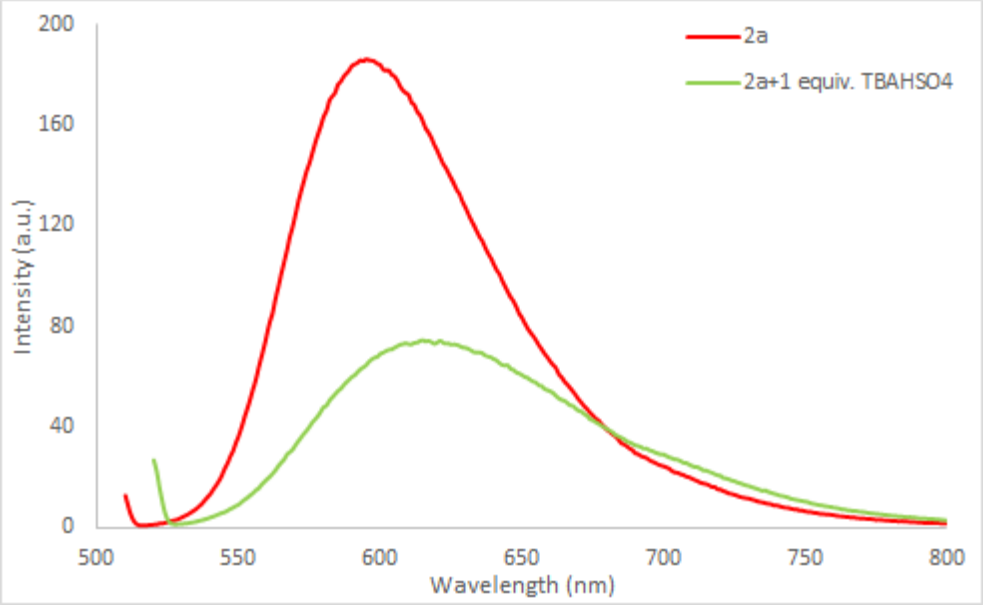

Figure S29. Fluorescence emission spectrum of **2a** upon addition of $TBA^{+}HSO_4^{-}$. λ_{ex} red= 506.5 nm, λ_{ex} green= 518.5 nm.

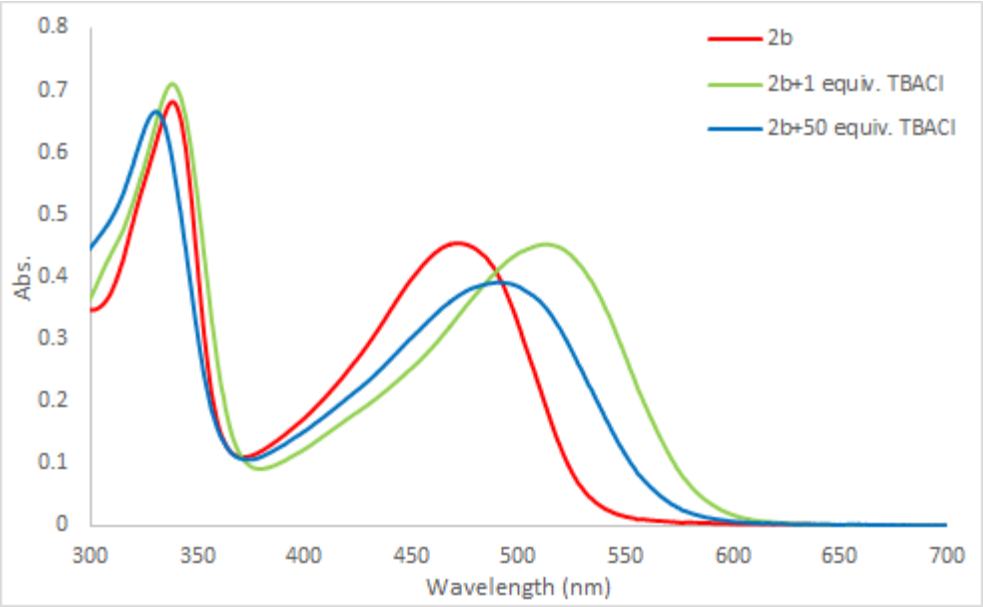

Figure S30. UV-Vis absorption spectrum of **2b** upon addition of $TBA^{+}Cl^{-}$.

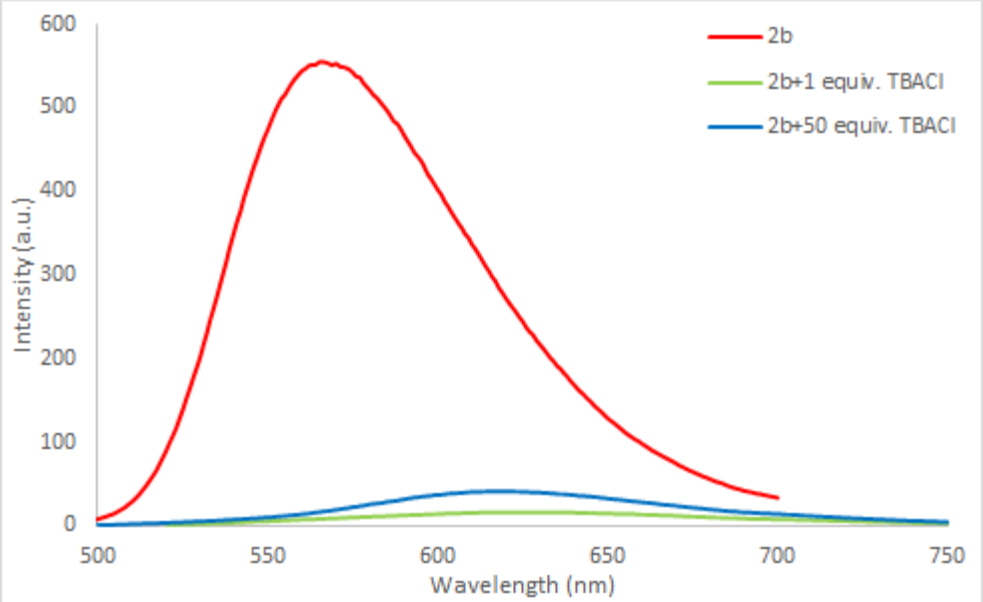

Figure S31. Fluorescence emission spectrum of **2b** upon addition of $TBA^{+}Cl^{-}$.
λ_{ex} red= 472 nm, λ_{ex} green= 513 nm, λ_{ex} blue= 492.5 nm.

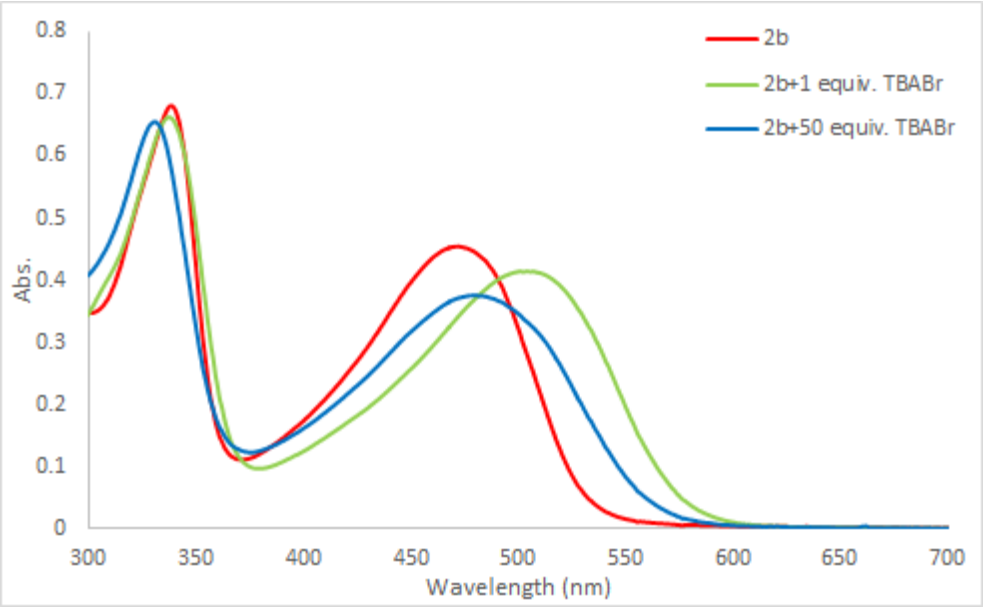

Figure S32. UV-Vis absorption spectrum of **2b** upon addition of $TBA^{+}Br^{-}$.

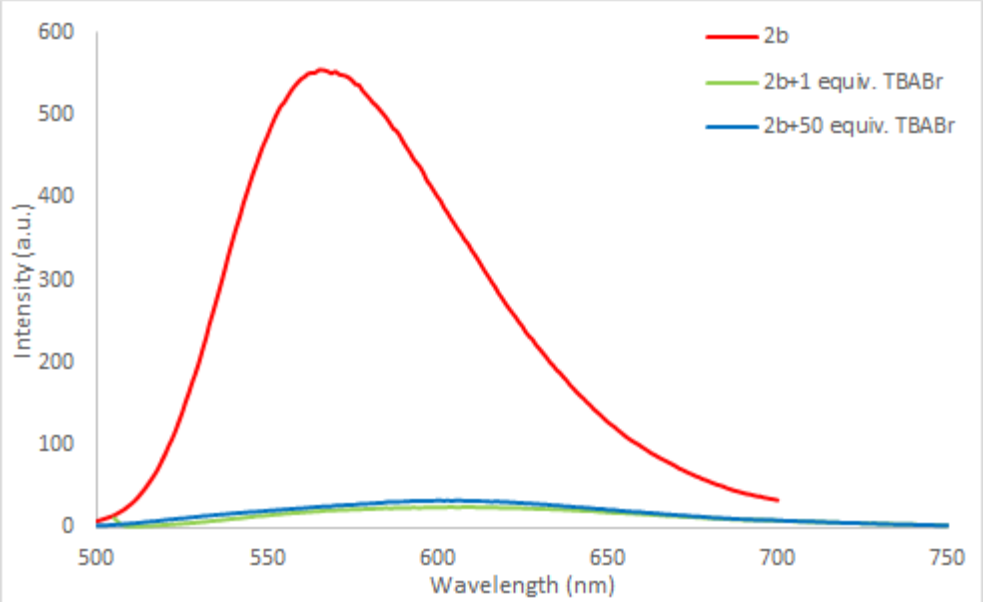

Figure S33. Fluorescence emission spectrum of **2b** upon addition of $TBA^{+}Br^{-}$. λ_{ex} red= 472 nm, λ_{ex} green= 501 nm, λ_{ex} blue= 480 nm.

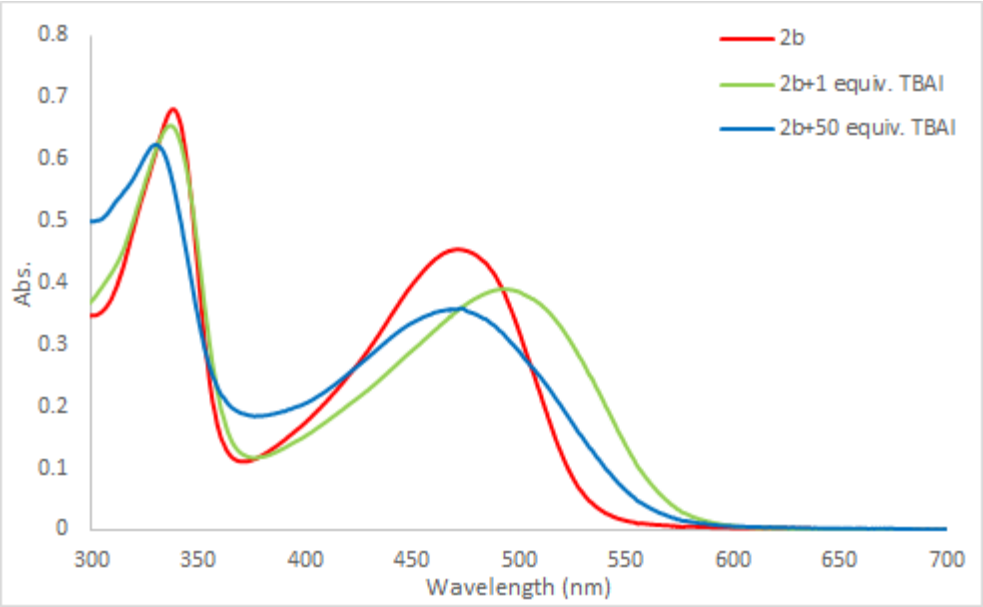

Figure S34. UV-Vis absorption spectrum of **2b** upon addition of $TBA^{+}I^{-}$.

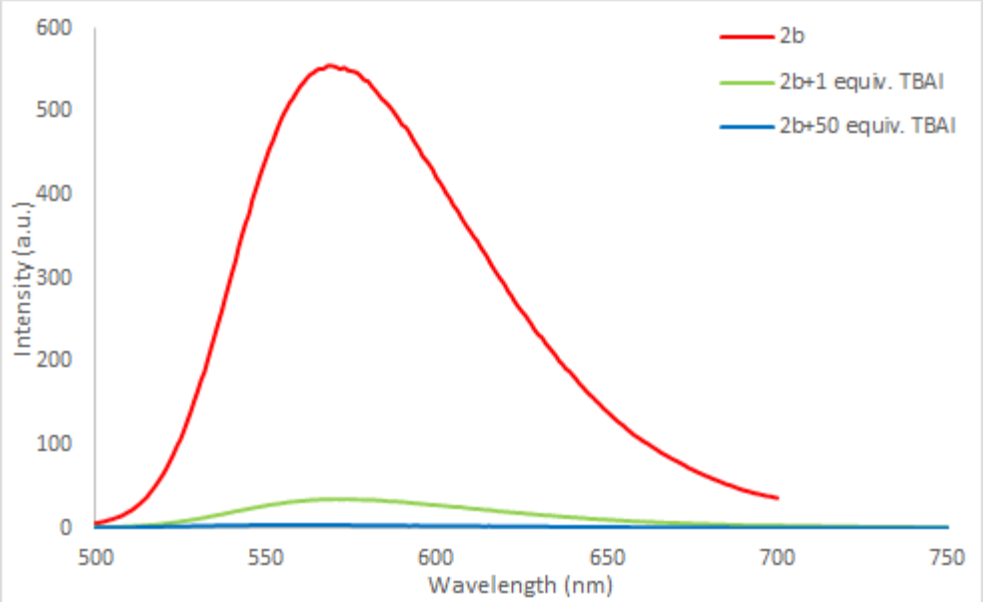

Figure S35. Fluorescence emission spectrum of **2b** upon addition of $TBA^{+}I^{-}$.
λ_{ex} red= 472 nm, λ_{ex} green= 493.5 nm, λ_{ex} blue= 472.5 nm.

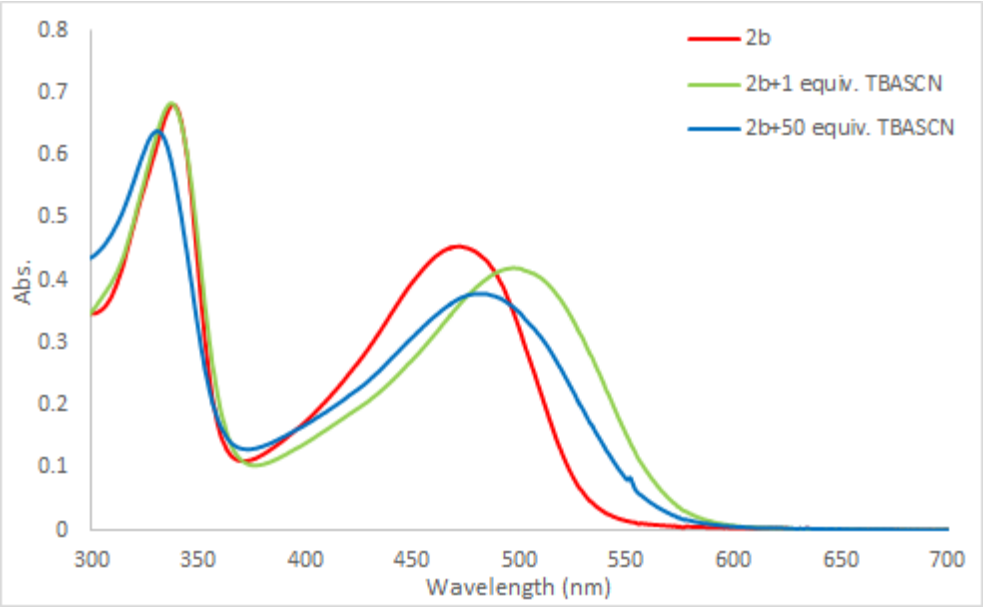

Figure S36. UV-Vis absorption spectrum of **2b** upon addition of $TBA^{+}SCN^{-}$.

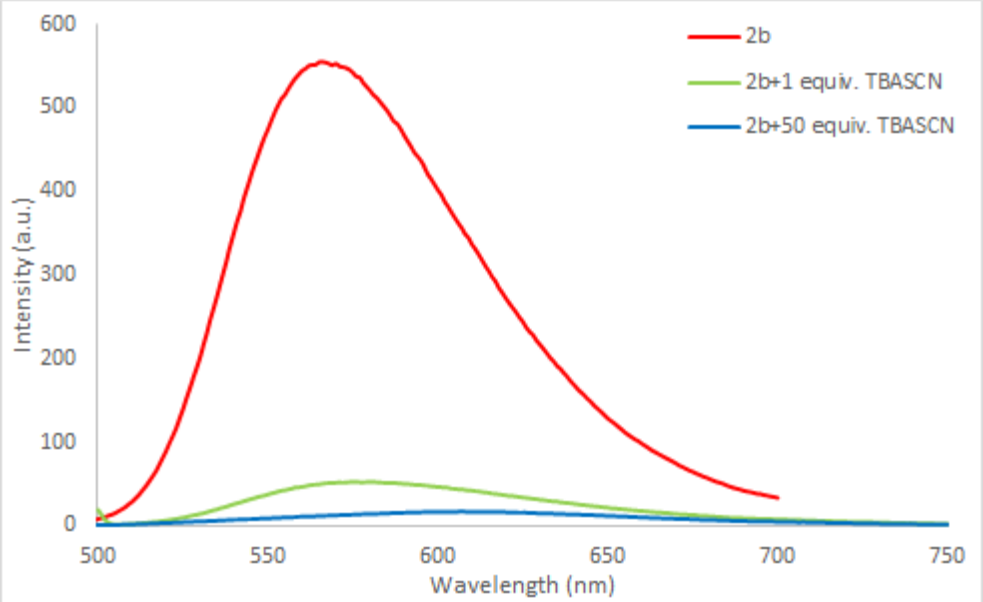

Figure S37. Fluorescence emission spectrum of **2b** upon addition of $TBA^{+}SCN^{-}$. λ_{ex} red= 472 nm, λ_{ex} green= 497 nm, λ_{ex} blue= 481 nm.

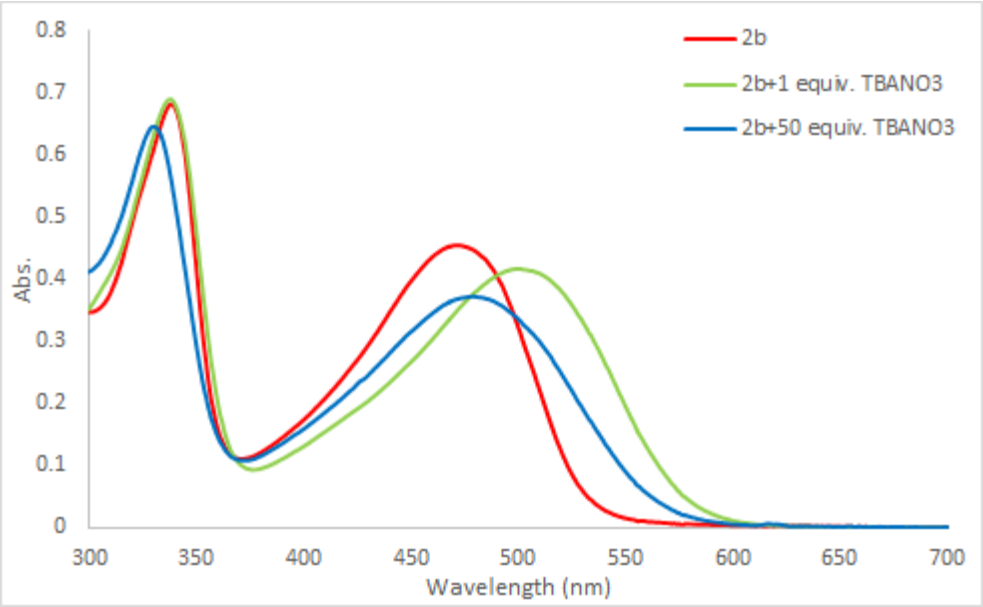

Figure S38. UV-Vis absorption spectrum of **2b** upon addition of $TBA^{+}NO_3^{-}$.

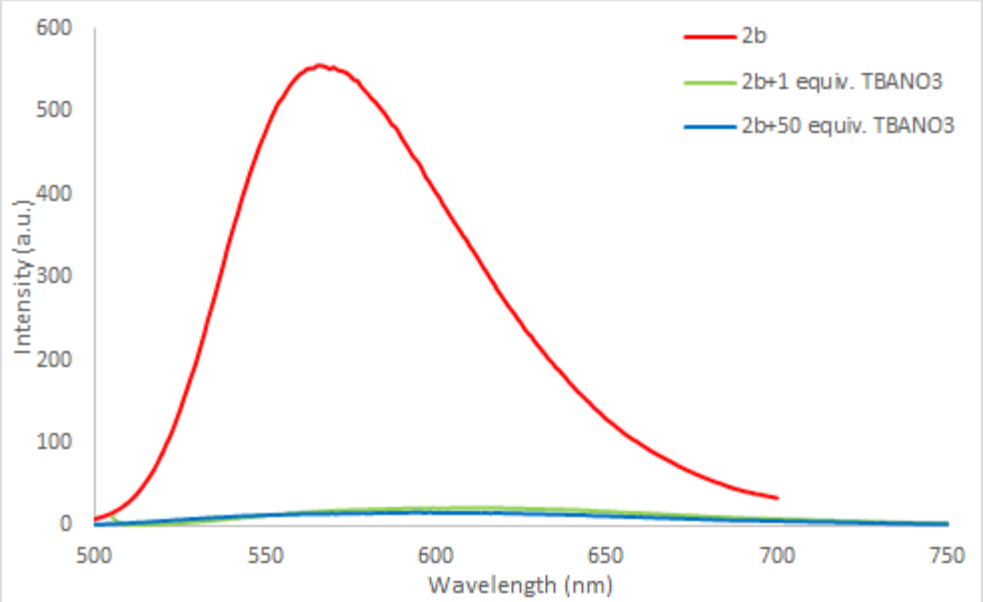

Figure S39. Fluorescence emission spectrum of **2b** upon addition of $TBA^{+}NO_3^{-}$. λ_{ex} red= 472 nm, λ_{ex} green= 501 nm, λ_{ex} blue= 478.5 nm.

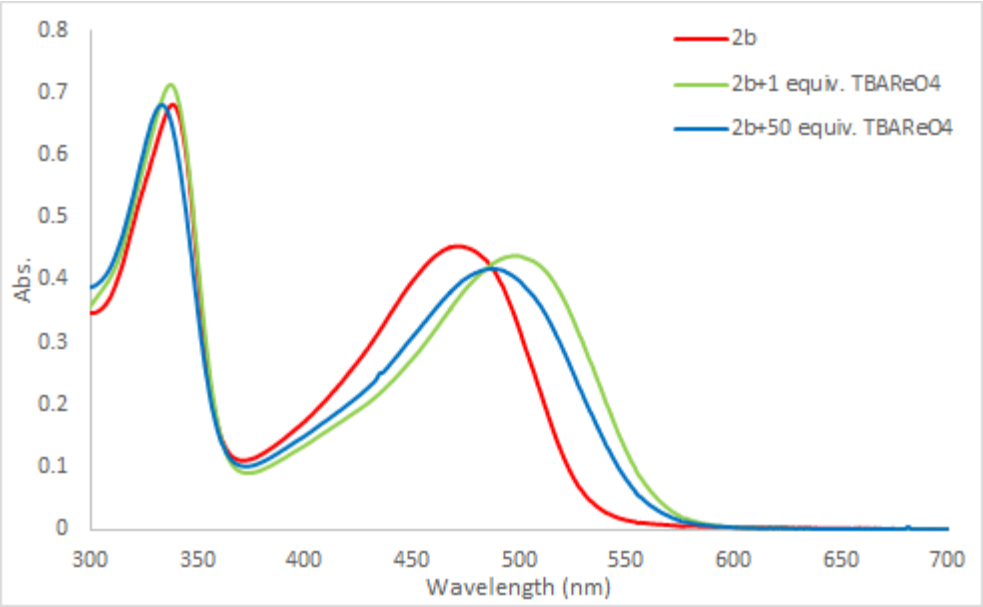

Figure S40. UV-Vis absorption spectrum of **2b** upon addition of $TBA^{+}ReO_4^{-}$.

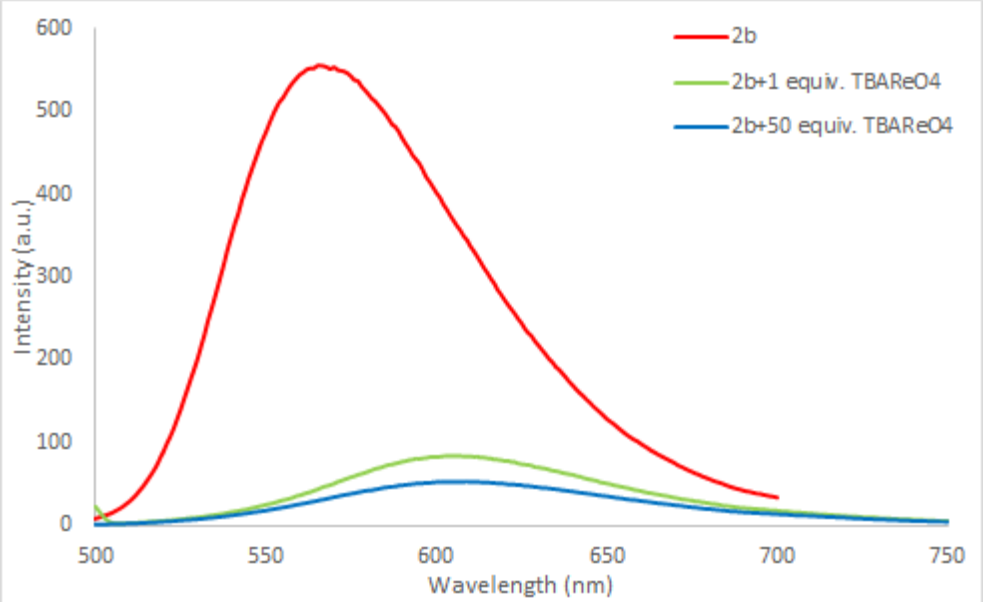

Figure S41. Fluorescence emission spectrum of **2b** upon addition of $TBA^{+}ReO_4^{-}$. λ_{ex} red= 472 nm, λ_{ex} green= 499 nm, λ_{ex} blue= 488 nm.

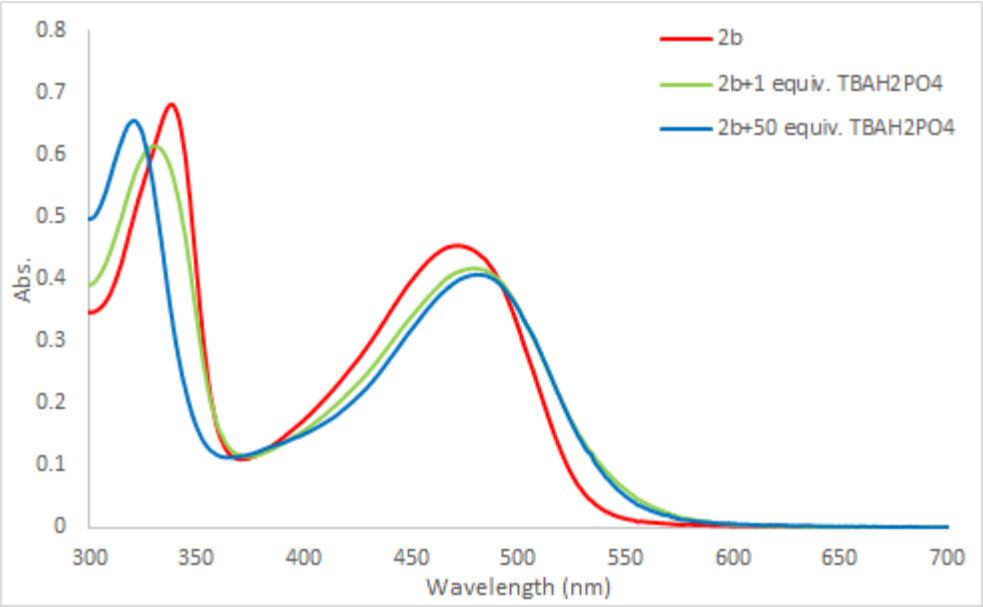

Figure S42. UV-Vis absorption spectrum of **2b** upon addition of $TBA^{+}H_2PO_4^{-}$.

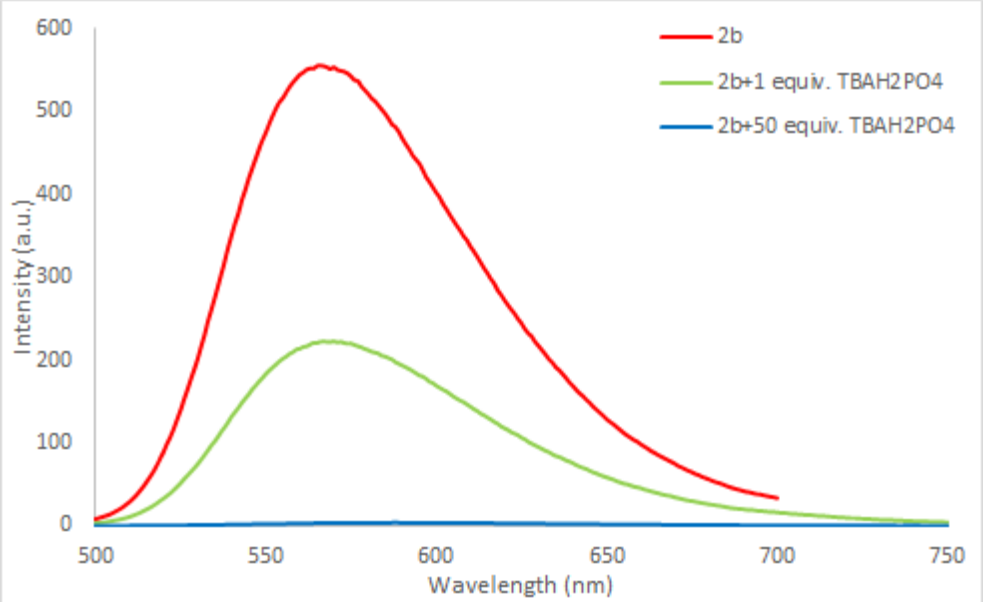

Figure S43. Fluorescence emission spectrum of **2b** upon addition of $TBA^{+}H_2PO_4^{-}$. λ_{ex} red= 472 nm, λ_{ex} green= 479 nm, λ_{ex} blue= 481 nm.

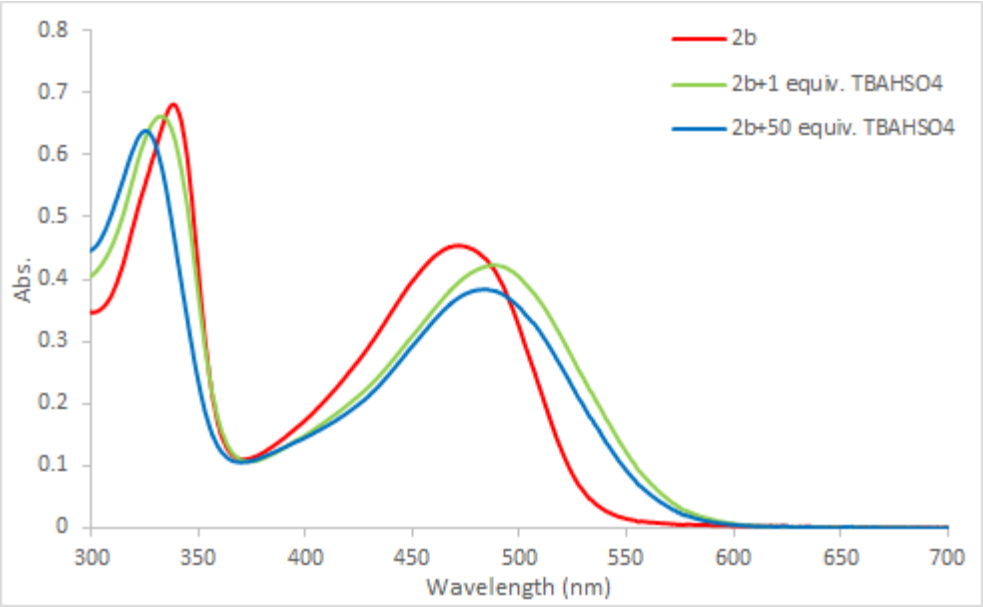

Figure S44. UV-Vis absorption spectrum of **2b** upon addition of $TBA^{+}HSO_4^{-}$.

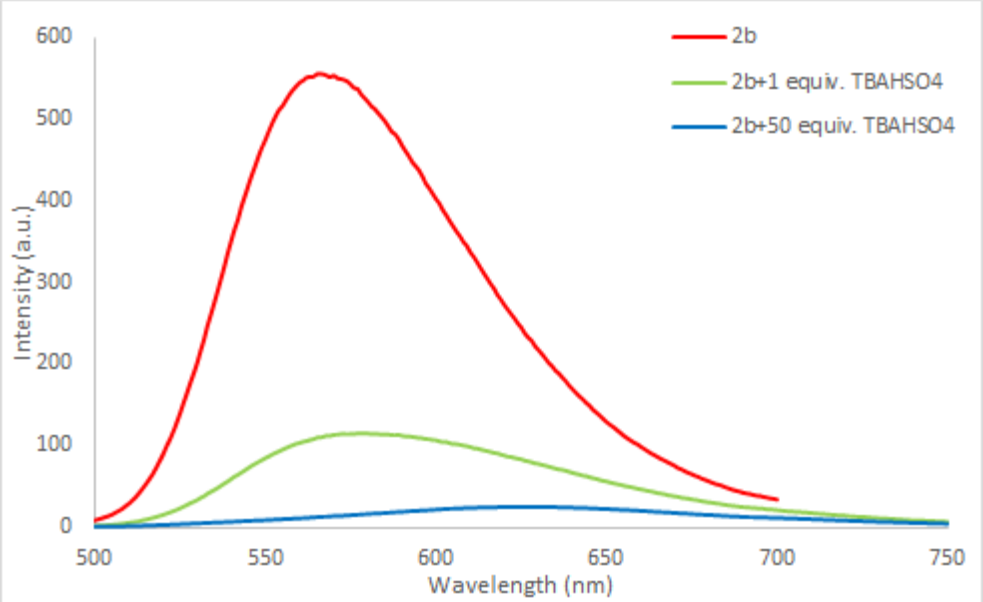

Figure S45. Fluorescence emission spectrum of **2b** upon addition of $TBA^{+}HSO_4^{-}$. λ_{ex} red= 472 nm, λ_{ex} green= 488 nm, λ_{ex} blue= 484 nm.

F. Synthetic details

General:

All materials were obtained from Sigma-Aldrich, Acros, TCI-America and Strem Chemcials and used without further purification. Nuclear Magnetic Resonance ^{1}H NMR, ^{13}C NMR and ^{19}F NMR spectra were recorded on Varian Direct Drive 500 MHz and Bruker Avance 400 MHz spectrometers. Chemical shifts (δ) expressed as ppm. For the ^{19}F NMR spectra C_6F_6 (δ -164.9 ppm) was used as an internal standard. Signal splitting patterns are indicated as s, singlet; d, doublet; t, triplet; m, multiplet, b, broad. Coupling constants (*J*) are given in Hz. Compounds were analyzed via HPLC-qToF-MS to obtain accurate mass data.

General procedure for anion metathesis of triflate salt to chloride salt. Octylated triflate salt of **4** or **5** was dissolved in the smallest amount of acetonitrile (enough to solubilize the receptor salt but not dilute it). 2.2 equivalents of tetra-*n*-butylammonium chloride were added to the acetonitrile mixture. Red precipitate formed upon addition of TBACl, reaction was stirred overnight at room temperature. Precipitate was gravity filtered. ^{1}H and ^{19}F NMR showed precipitate was clean product and no further purification was needed.

Procedures for alkylation and BArF metathesis were conducted as previously reported (Massena, C. J., Riel, A. M. S., Neuhaus, G. F., Decato, D. A., & Berryman, O. B. (**2015**). Chemical Communications, 51(8), 1417-1420.)

Figure S46. Synthetic Pathway

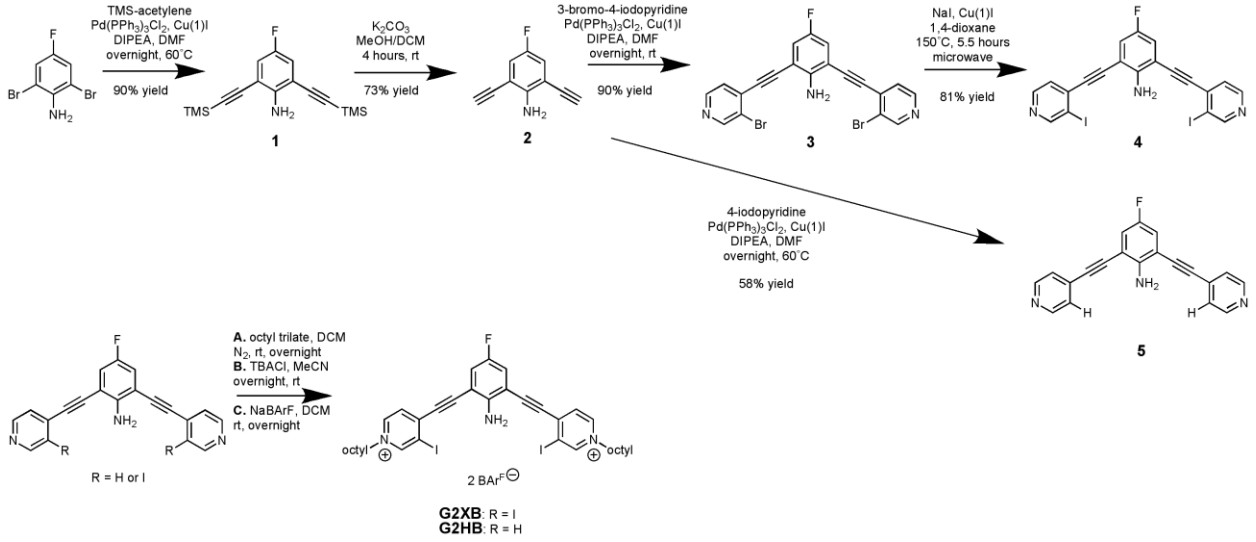

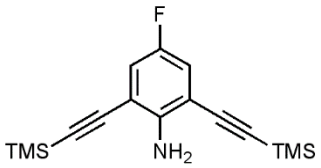

4-fluoro-2,6-bis((trimethylsilyl)ethynyl)aniline (1). To an oven dried Schlenk flask was charged with 2,6-dibromo-4-fluoroaniline (4.9787 g, 18.51 mmol), then vacuumed and backfilled with dry N_2 gas (3x). Bis(triphenylphosphine)palladium(II) dichloride (0.778 g, 1.10 mmol) was added, vacuumed and backfilled with dry N_2 (3x). Copper (I) iodide (0.354 g, 1.86 mmol) was added, vacuumed and backfilled with dry N_2 (3x). The dry reagents were dissolved in 150 mL dry dimethylformamide (DMF). N,N-diisopropylamine (16 mL, 91.85 mmol) and TMS-acetylene (6.65 mL, 46.56 mmol) were added to the DMF solution. The flask was carefully vacuumed and backfilled with dry N_2 (3x). The dark brown solution stirred overnight at 60˚C. The reaction mixture was first run through a silica plug with a hexane/ethyl acetate solvent mixture (50:50) to remove any excess salts and catalysts. Subsequent removal of DMF, hexanes and ethyl acetate by roto-evaporation left a brown solid that was purified by column chromatography (gradient column of pure hexanes to 5% EtOAc/95% Hexanes) to afford **1** (5.04 g, 16.6 mmol, 90%) as a golden yellow colored oil. ^{1}H (400 MHz, $CDCl_3$, 25˚C): 6.9916-6.9697 (2H, d, *J* = 8.76 Hz), 4.6717 (2H, s), 0.2598 (18H, s). ^{13}C (125.7 MHz, $CDCl_3$, 25˚C): 154.7221-152.8471 (d, *J* = 235.7 Hz), 146.8236, 119.3367 (d, *J* = 23.9 Hz), 108.0455 (d, *J* = 9.7 Hz), 101.5135, 100.2913, 0.1138. ^{19}F (470.6 MHz, $CDCl_3$, 25˚C): -130.7549 (1F, t, *J* = 8.73 Hz). HRMS (ESI pos) *m/z*: 304.1353 (M^++1, 100%); $C_{16}H_{23}FNSi_2^+$+1 (304.1377).

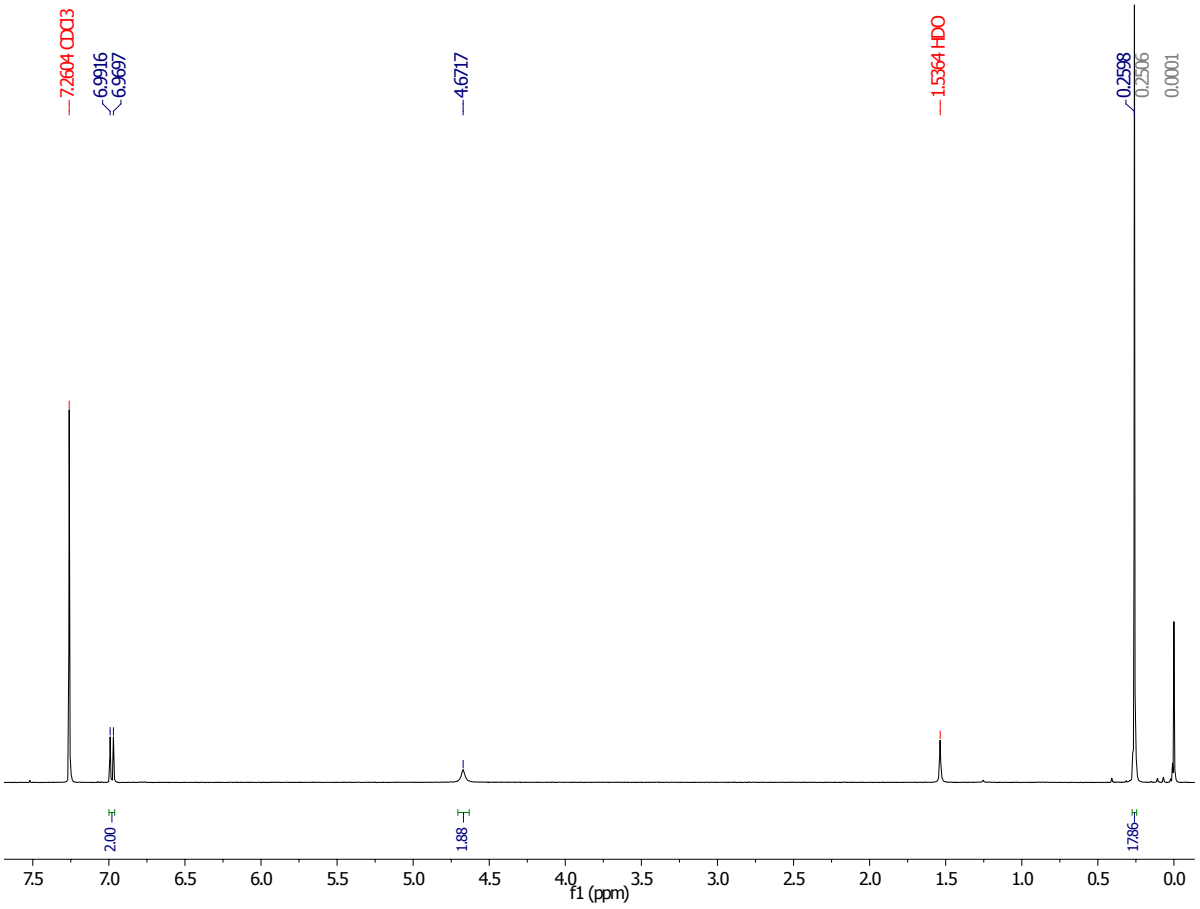

Figure S47. ^{1}H NMR of spectrum of **1** ($CDCl_3$, 25˚C, 400 MHz).

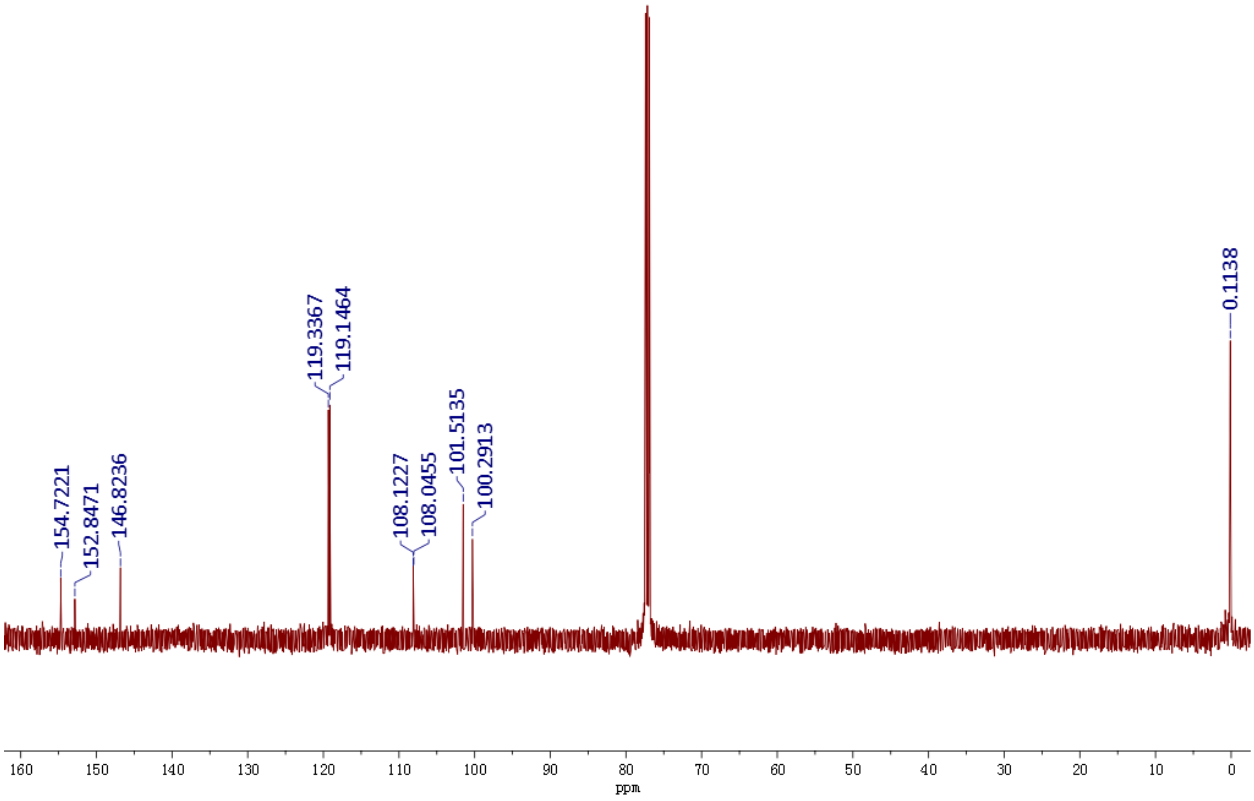

Figure S48. ^{13}C NMR of spectrum of **1** ($CDCl_3$, 25˚C, 125.7 MHz).

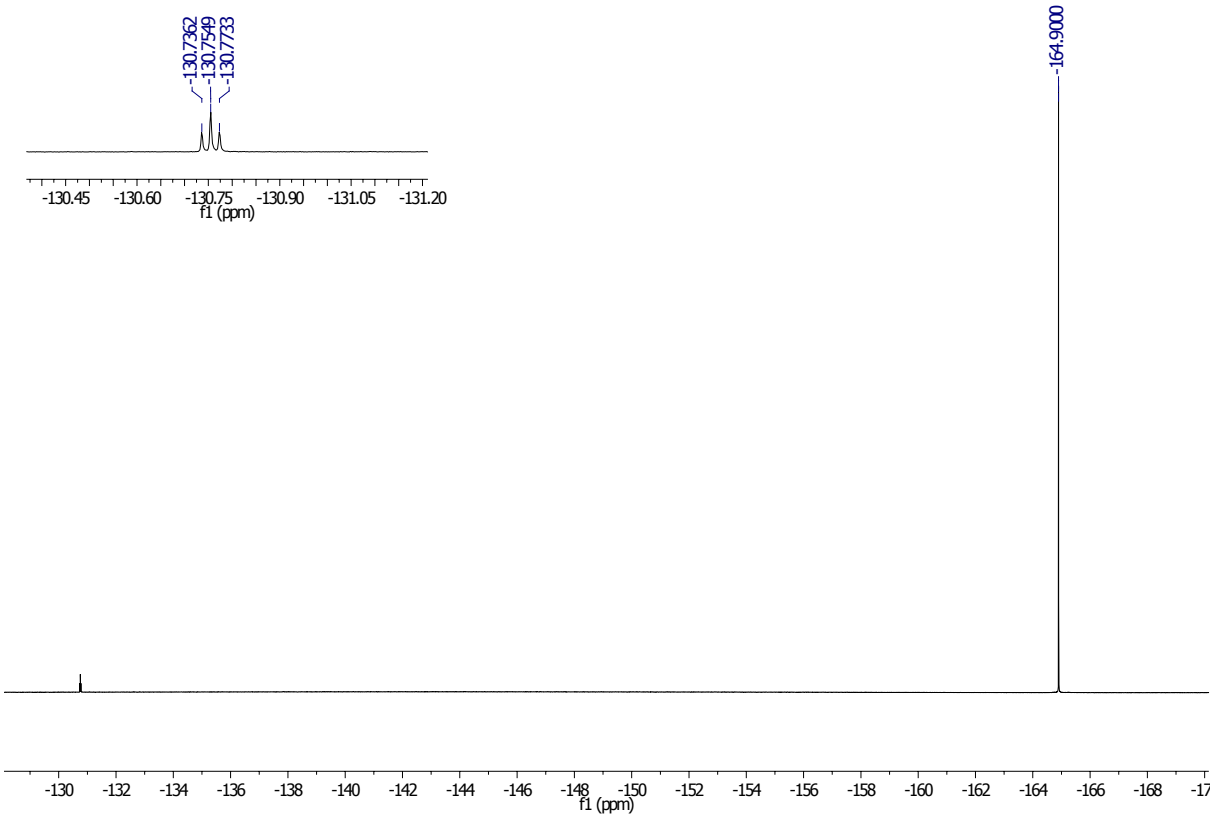

Figure S49. ^{19}F NMR of spectrum of **1** ($CDCl_3$, 25˚C, 470.6 MHz).

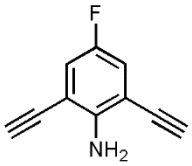

2,6-bisethynyl-4-fluoroaniline (2). 1 (1.59 g, 5.24 mmol) was dissolved in 15 mL methanol and 15 mL DCM in a 250 mL round bottom flask. Potassium carbonate (1.85 g, 13.11 mmol) was added to the organic mixture. The reaction stirred vigorously for 4 hours at room temperature and reaction progress was checked via TLC. If the reaction was not finished, it was stirred overnight. When the reaction came to completion, water was added to quench the reaction. The crude product was extracted with ethyl acetate, dried over magnesium sulfate and vacuum filtered. The organic mixture was reduced under vacuum and crude product remained a brown solid. The clean yellow solid **2** (0.610 g, 73 % yield) was obtained by column chromatography (10% DCM/90 % Hexanes). ^1H (400 MHz, $CDCl_3$, 25˚C): 7.0602-7.0387 (2H, d, *J* = 8.6 Hz), 4.7013 (2H, s), 3.4343 (2H, s). ^{13}C (125.7 Hz, $CDCl_3$, 25˚C): 154.6664-152.7916 (d, *J* = 235.7 Hz), 147.2792, 120.1869 (d, *J* = 24.1 Hz), 107.0369 (d, *J* = 9.8 Hz), 83.8922, 79.2389. ^{19}F (470.6 MHz, $CDCl_3$, 25˚C): -130.5275 (1F, t, *J* = 8.66 Hz). HRMS (ESI pos) *m/z*: 160.0563 (M^++1, 100%); $C_{10}H_7FN^+$+1 (160.0563).

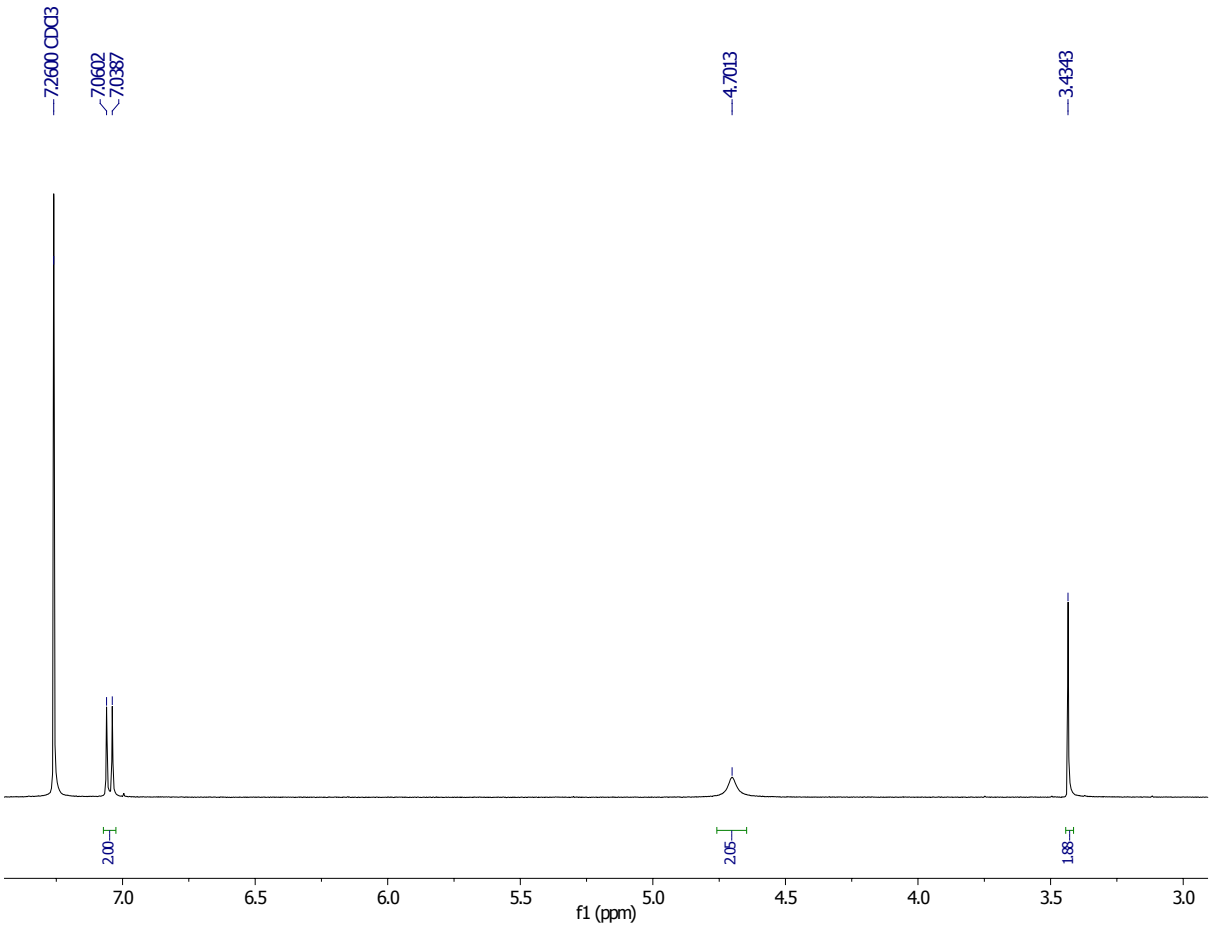

Figure S50. ^{1}H NMR of spectrum of **2** ($CDCl_3$, 25˚C, 400 MHz).

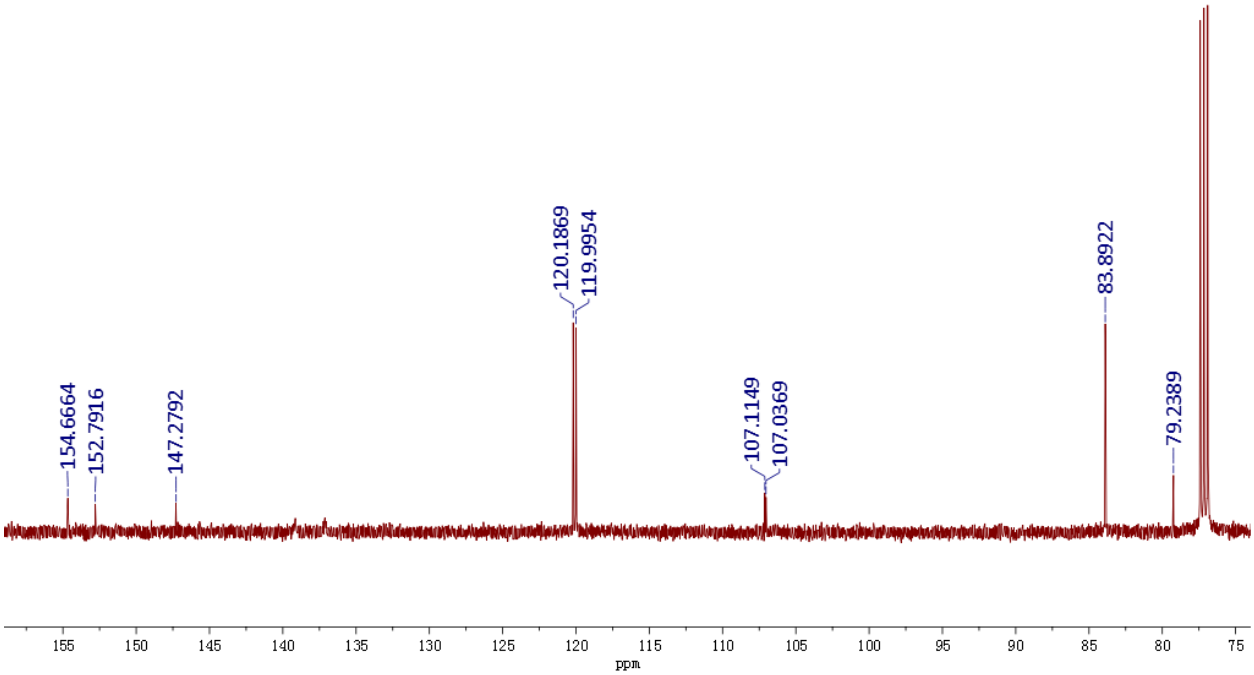

Figure S51. ^{13}C NMR of spectrum of **2** ($CDCl_3$, 25˚C, 125.7 MHz).

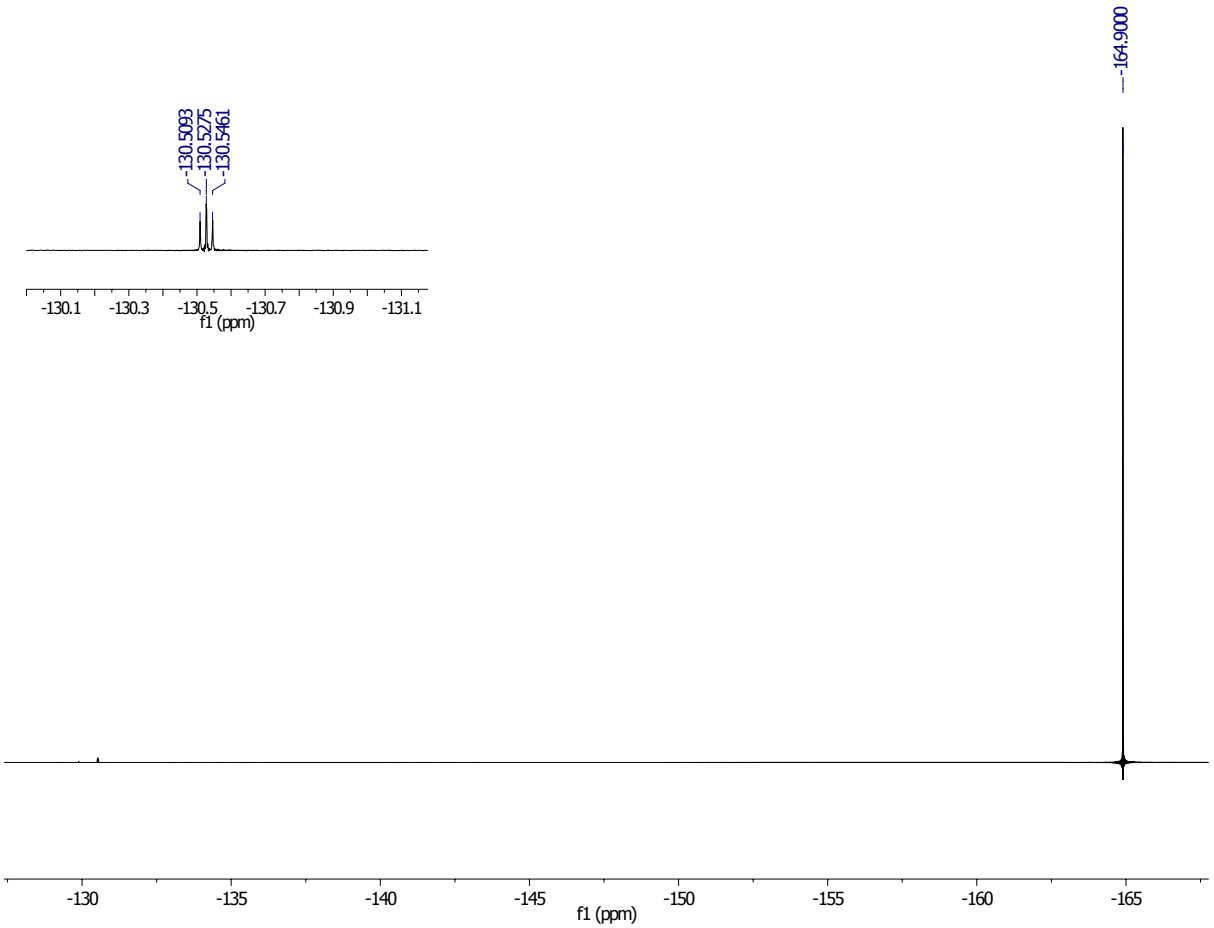

Figure S52. ^{19}F NMR of spectrum of **2** ($CDCl_3$, 25˚C, 470.6 MHz).

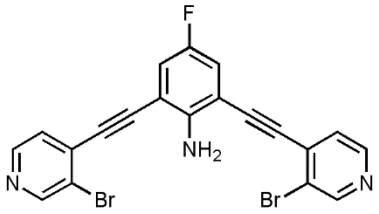

2,6-bis(4-ethynyl-3-bromopyridinyl)-4-fluoroaniline (3). To an oven dried Schlenk flask was charged with **2** (0.300 g, 1.88 mmol) and 4-bromo-3-iodopyridine (1.125 g, 4.71 mmol) then vacuumed and backfilled with dry N_2 gas (3x). Bis(triphenylphosphine)palladium (II) dichloride (0.0793 g, 0.113 mmol) was added, vacuumed and backfilled with dry N_2 (3x). Copper (I) iodide (0.035 g, 0.188 mmol) was added, vacuumed and backfilled with dry N_2 (3x). The dry reagents were dissolved in 60 mL dry DMF. N,N-diisopropylamine (1.6 mL, 9.4 mmol) was added to the DMF solution. The flask was carefully vacuumed and backfilled with dry N_2 (3x). The dark brown solution stirred overnight at room temperature. The reaction mixture was first run through a silica plug with a hexane/ethyl acetate solvent mixture (50:50) to remove any excess salts and catalysts. Subsequent removal of DMF, hexanes and ethyl acetate by roto-evaporation left and brown solid that was purified by column chromatography (gradient from 30% EtOAc/70% Hexanes to 75% EtOAc/25% Hexanes) to afford **3** (5.04 g, 16.6 mmol, 90%) as a bright yellow solid. ^1H (400 MHz, $CDCl_3$, 25˚C): 8.8199 (2H, s), 8.5531-8.5406 (2H,

d, *J* = 5 Hz), 7.4405-7.4280 (2H, d, *J* = 5 Hz), 7.2255-7.2045 (2H, d, *J* = 8.4 Hz), 5.2456 (2H, s). ^{13}C (125.7 MHz, CDCl3, 25˚C): 155.42, 153.07-152.16 (d, *J* = 114.4 Hz), 148.43, 133.02, 132.69, 126.81, 123.06, 121.46 (d, *J* = 30.2 Hz), 107.77 (d, *J* = 43.0 Hz), 94.45, 92.76. ^{19}F (470.6 MHz, $CDCl_3$, 25˚C): -129.9064 (1F, t, *J* = 8.35 Hz). HRMS (ESI pos) *m/z*: 471.9283 (M^++1, 100%); $C_{20}H_{11}Br_2FN_3^+$+1 (471.9350).

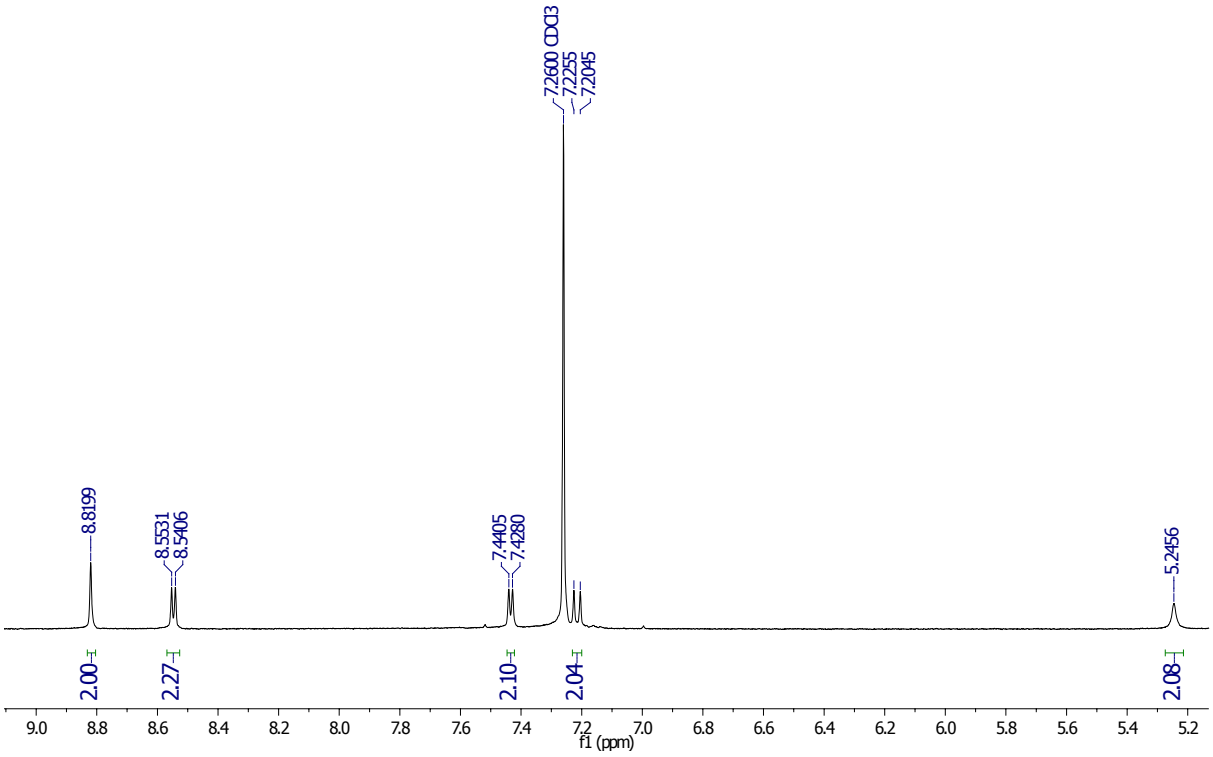

Figure S53. ^{1}H NMR of spectrum of **3** ($CDCl_3$, 25˚C, 400 MHz).

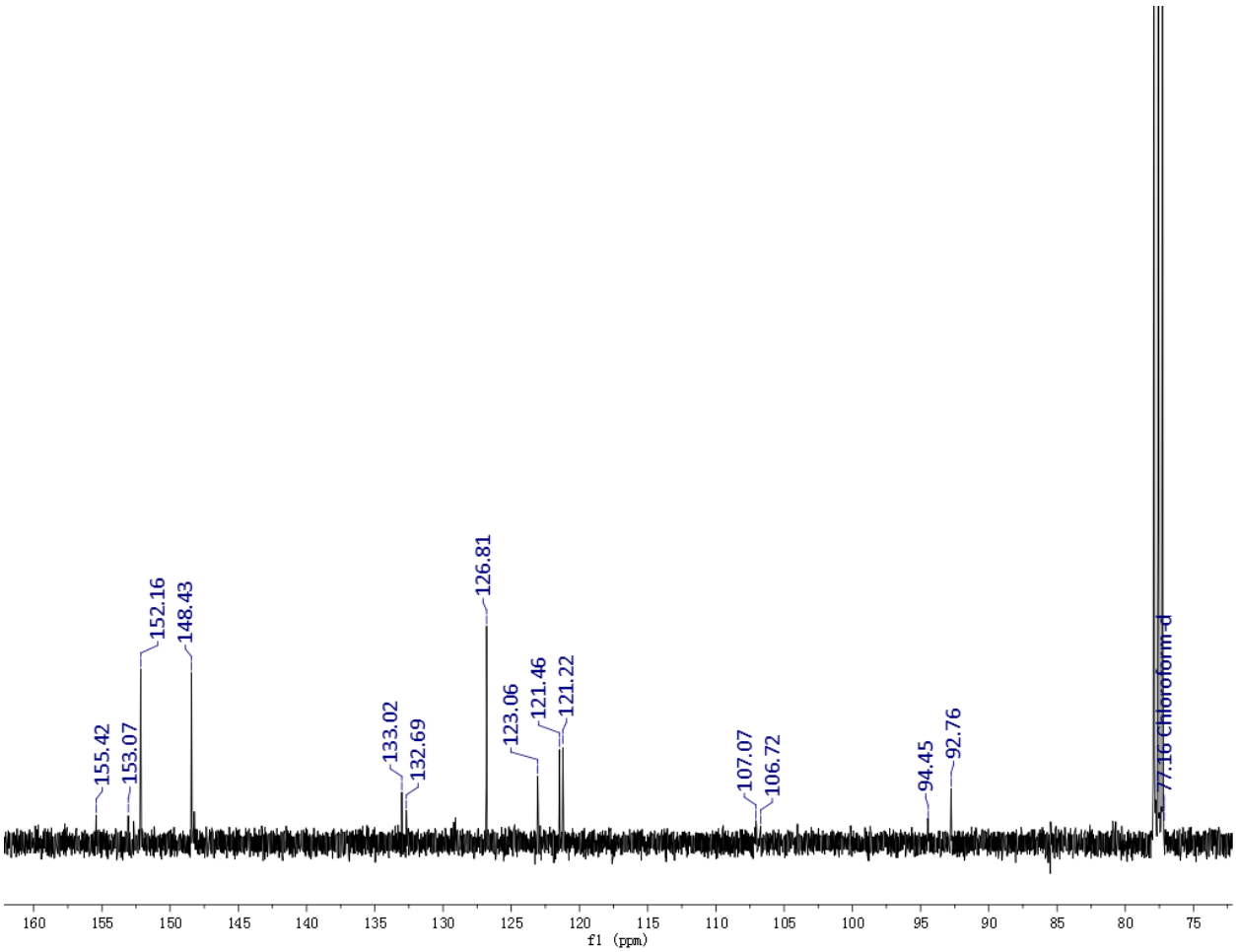

Figure S54. ^{13}C NMR of spectrum of **3** ($CDCl_3$, 25˚C, 125.7 MHz).

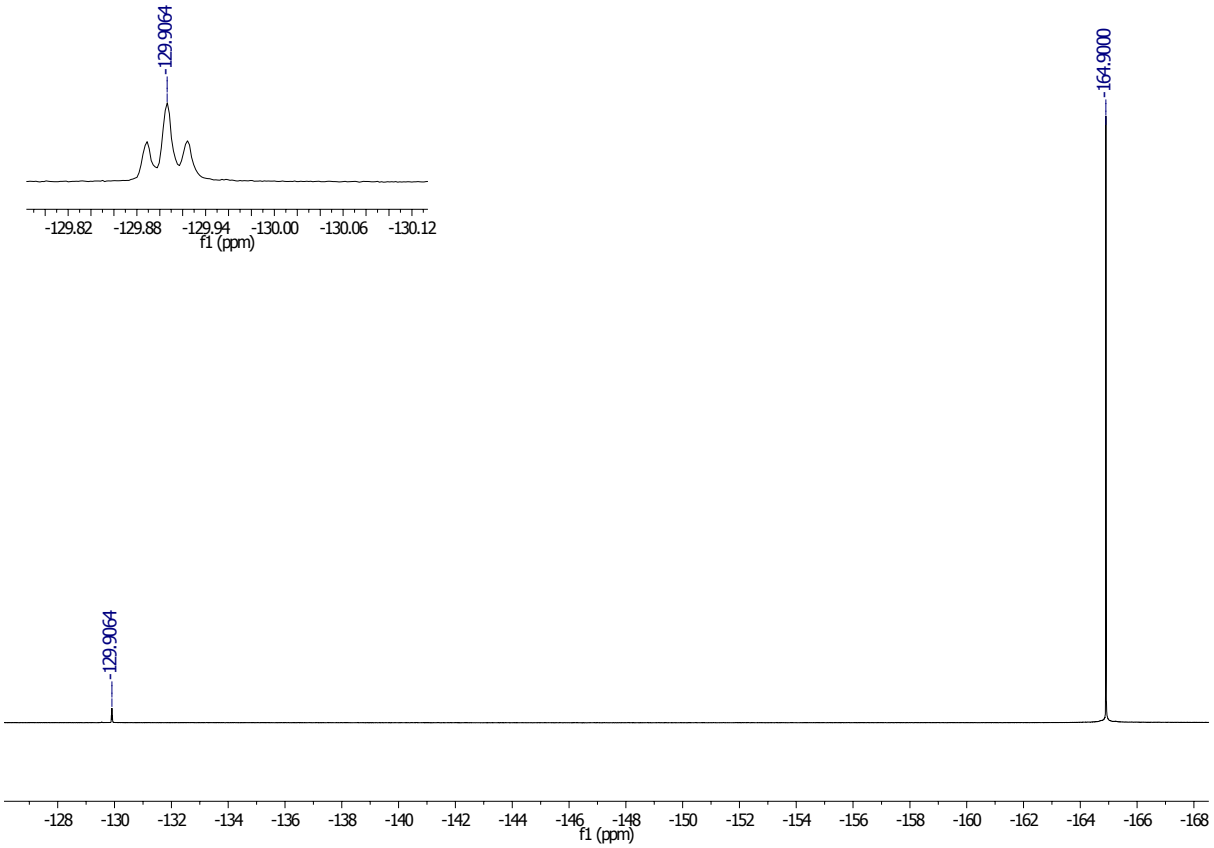

Figure S55. ^{19}F NMR of spectrum of **3** ($CDCl_3$, 25˚C, 470.6 MHz).

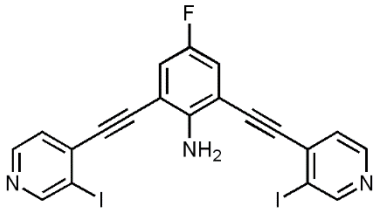

2,6-bis(4-ethynyl-3-iodopyridinyl)-4-fluoroaniline (4). 3 (0.225 g, 0.47 mmol), copper iodide (0.009 g, 0.047 mmol), sodium iodide (0.286 g, 1.91 mmol) were added to a 10-20 mL microwave reaction vial containing a stir bar and dissolved in 13 mL 1,4-dioxane. To the vibrant yellow reaction mixture, trans-N,N'-dimethylcyclohexane-1,2-diamine (0.23 mL, 1.45 mmol) was added which turned the solution color green-brown. The microwave vial was sealed and placed in a microwave. The reaction was performed in a Biotage Initiator+ microwave reactor for 5.5 hours at 150 ˚C. After cooling, an aliquot was ran through pipet silica plug with EtOAc to remove catalysts and salts. The EtOAc crude was then ran through GCMS in order to obtain % conversion of bromines to iodines. If the reaction was unfinished, it would be submitted again at 30 min incriments. When the reaction ran to completion, the crude reaction was run through a silica plug with EtOAc. The bright yellow product (0.219 g, 0.39 mmol, 81%) was purified via column chromatography (gradient column 30% EtOAc/70% Hexanes to 70% EtOAc/30% Hexanes). ^1H (400 MHz, $CDCl_3$, 25˚C): 9.0073 (2H, s),

8.5603-8.5478 (2H, d, *J* = 5 Hz), 7.4334-7.4209 (2H, d, *J* = 5 Hz), 7.2380-7.21770 (2H, d, *J* = 8.4 Hz), 5.3240 (2H, s). ^{13}C (125.7 MHz, CDCl3, 25˚C): 157.1417, 154.7946-152.9078 (d, *J* = 237.2 Hz), 148.6974, 147.7629, 136.7807, 126.3512, 120.8622 (d, *J* = 24.0 Hz), 106.7141 (d, *J* = 9.7 Hz), 98.9006, 95.5187, 92.9690. ^{19}F (470.6 MHz, $CDCl_3$, 25˚C): -129.8910 (1F, t, *J* = 8.3 Hz). HRMS (ESI pos) *m/z*: 565.9026 (M^++1, 100%); $C_{20}H_{11}FI_2N_3^+$+1 (565.9040).

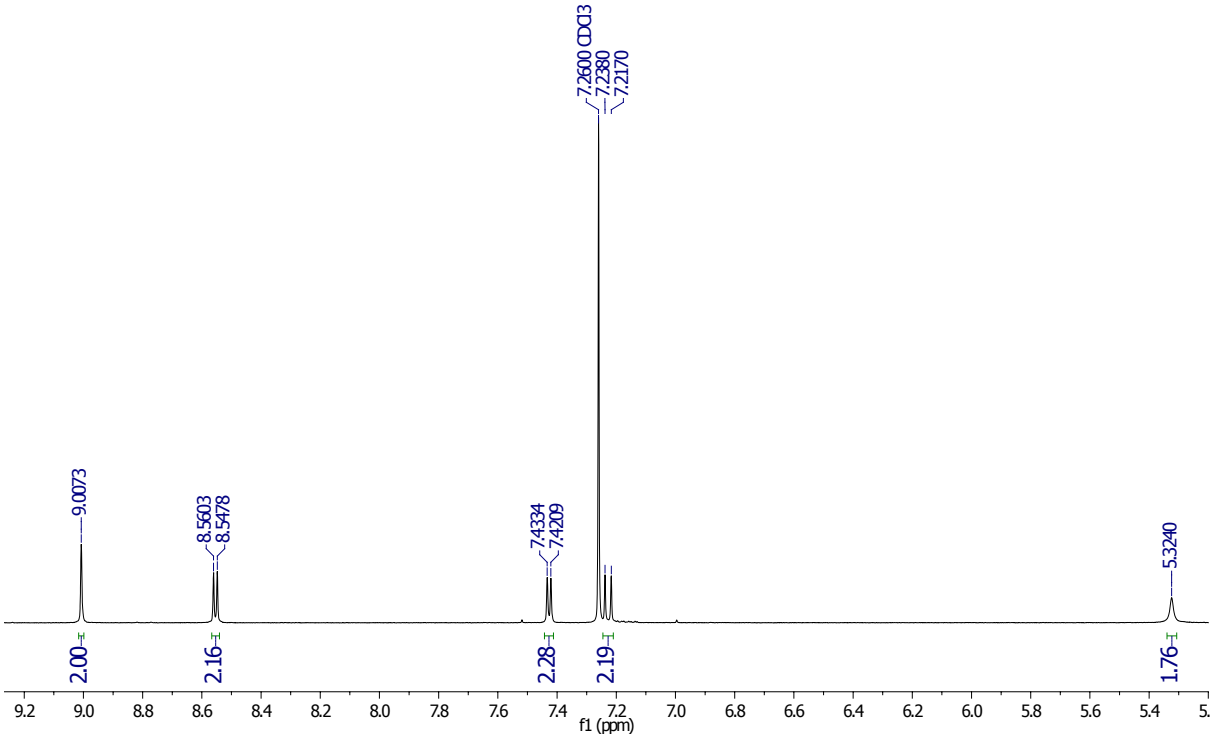

Figure S56. ^{1}H NMR of spectrum of **4** ($CDCl_3$, 25˚C, 400 MHz).

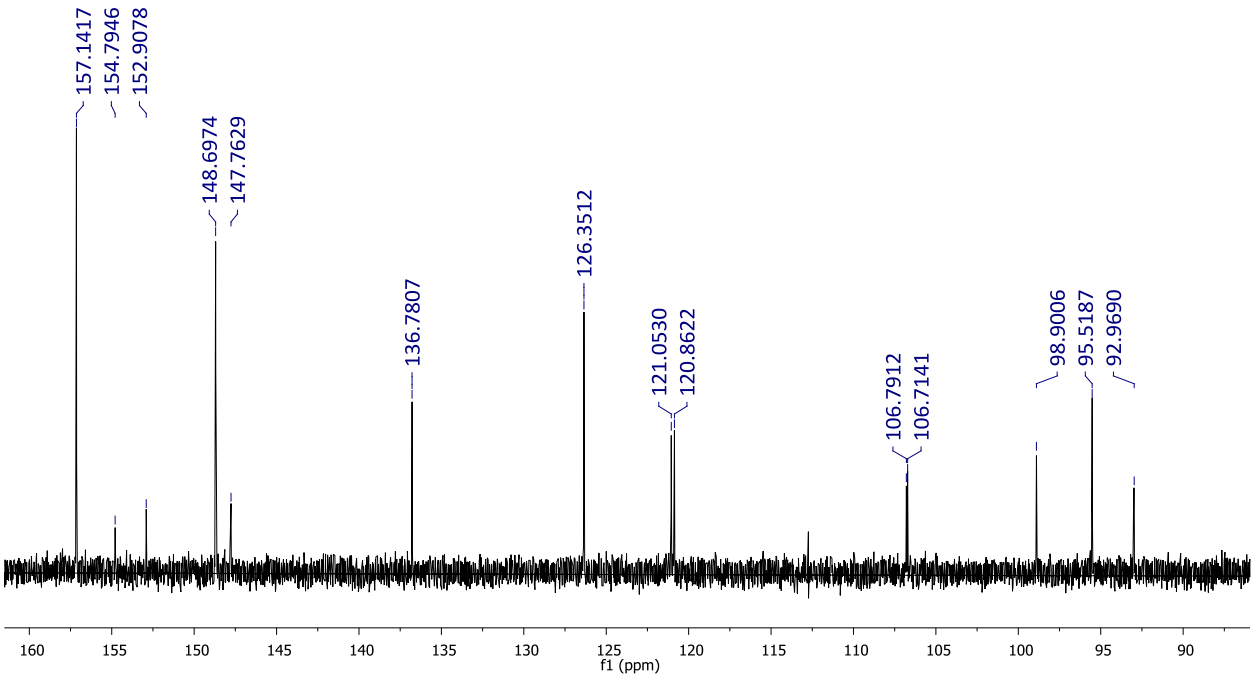

Figure S57. ^{13}C NMR of spectrum of **4** ($CDCl_3$, 25˚C, 125.7 MHz).

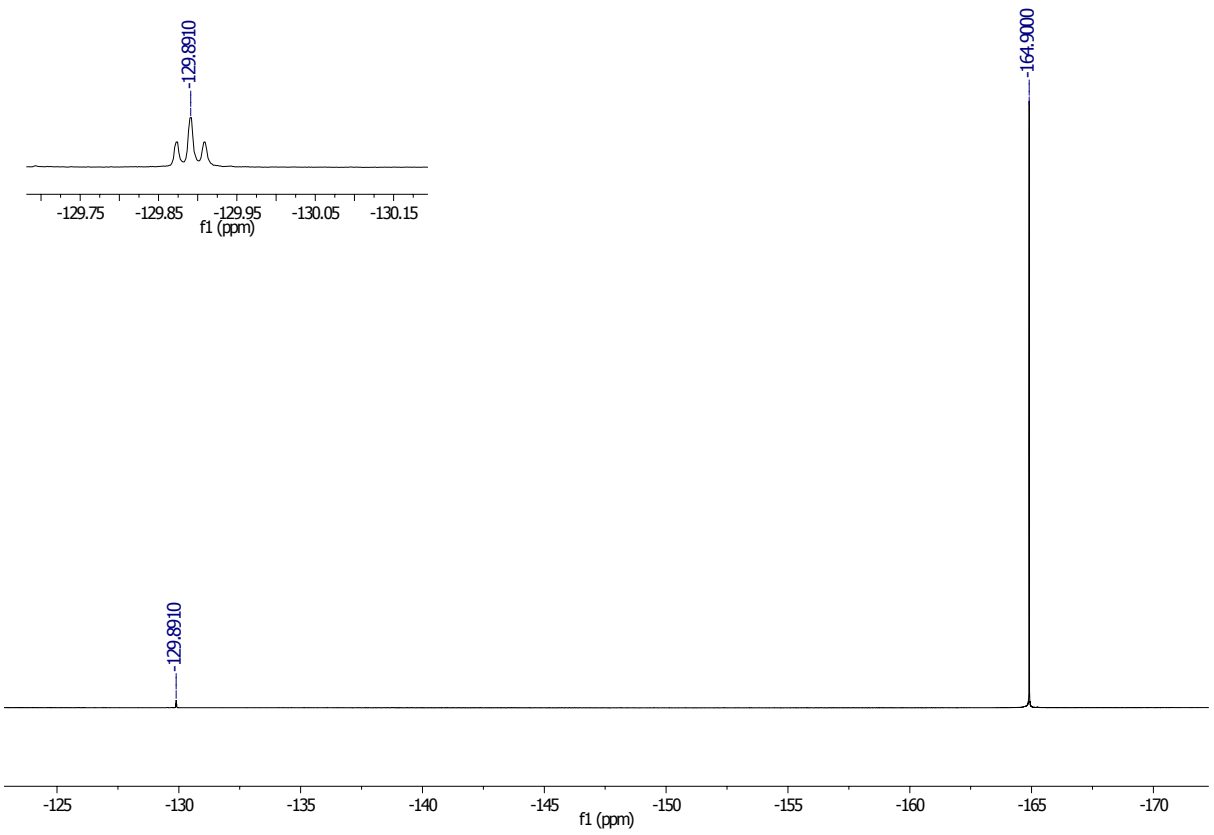

Figure S58. ^{19}F NMR of spectrum of **4** ($CDCl_3$, 25˚C, 470.6 MHz).

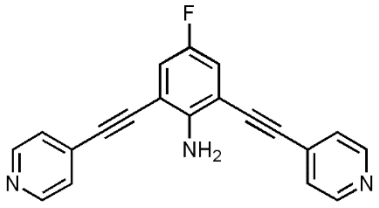

2,6-bis(4-ethynylpyridinyl)-4-fluoroaniline (5). To an oven dried Schlenk flask was charged with **2** (0.85 g, 5.34 mmol) and 4-iodopyridine (2.5 g, 12.2 mmol) then vacuumed and backfilled with dry N_2 gas (3x). Bis(triphenylphosphine)palladium (II) dichloride (0.226 g, 0.342 mmol) was added, vacuumed and backfilled with dry N_2 (3x). Copper (I) iodide (0.101 g, 0.53 mmol) was added, vacuumed and backfilled with dry N_2 (3x). The dry reagents were dissolved in 40 mL dry DMF. N,N-diisopropylamine (4.6 mL, 26.4 mmol) was added to the DMF solution. The flask was carefully vacuumed and backfilled with dry N_2 (3x). The dark brown solution stirred overnight at 150 ˚C. The reaction mixture was first run through a silica plug with an ethyl acetate/methanol solvent mixture (90:10) to remove any excess salts and catalysts. Subsequent removal of DMF, hexanes and ethyl acetate by roto-evaporation left and brown solid that was purified by column chromatography (gradient from 30% EtOAc/70% Hexanes to 75% EtOAc/25% Hexanes) to afford **5** (0.96 g, 3.1 mmol, 58%) as a bright yellow solid. ^1H (500 MHz, CD_3CN, 25˚C): 8.6234-8.6114 (2H, d, *J* = 6 Hz), 7.5059-74938

(4H, d, *J* = 6.05 Hz), 7.2422-7.2245 (2H, d, *J* = 8.85 Hz), 5.2600 (2H, s). ^{13}C (125.7 MHz, CD_3CN, 25˚C): 155.3862, 150.9501 (d, *J* = 6.9 Hz), 148.4883, 131.3914, 126.2978, 121.2470 (d, *J* = 24.2 Hz), 107.7302 (d, *J* = 10.13 Hz), 93.8579, 89.3999. ^{19}F (470.6 MHz, CD_3CN, 25˚C): -129.6846 (1F, t, *J* = 8.82 Hz). HRMS (ESI pos) *m/z*: 314.1094 (M^++1, 100%); $C_{20}H_{13}FN_3^+$+1 (314.1107).

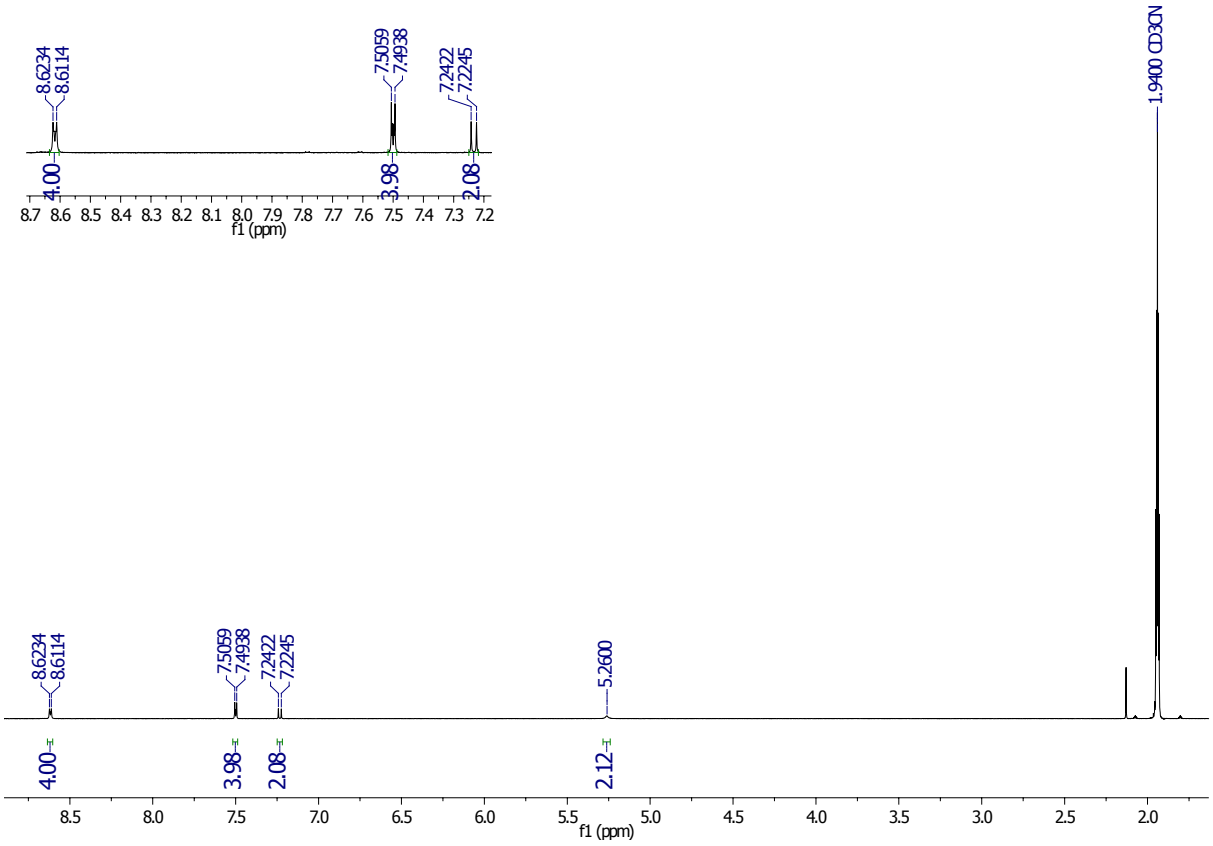

Figure S59. ^{1}H NMR of spectrum of **5** (CD_3CN, 25˚C, 500 MHz).

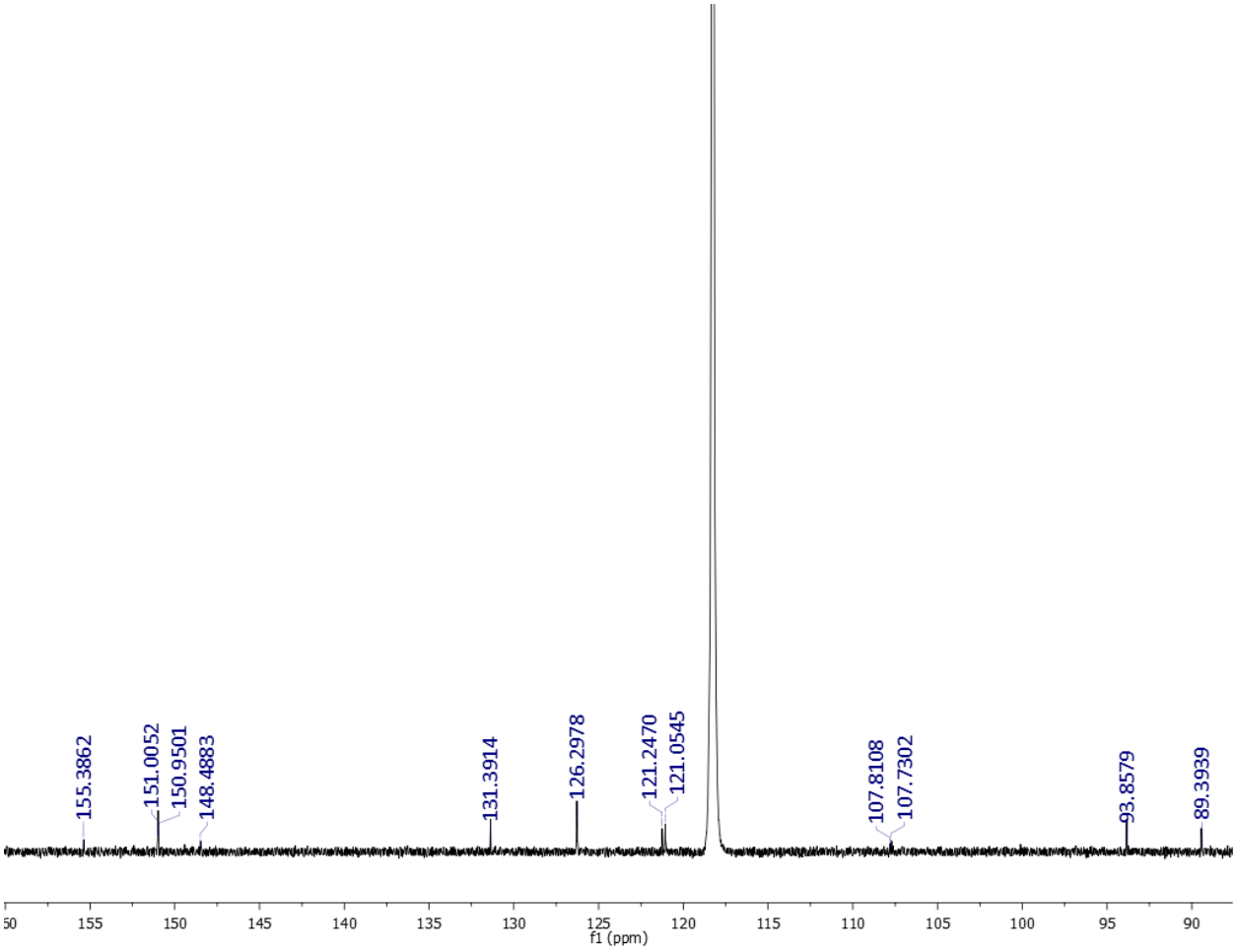

Figure S60. ^{13}C NMR of spectrum of **5** (CD_3CN, 25˚C, 125.7 MHz).

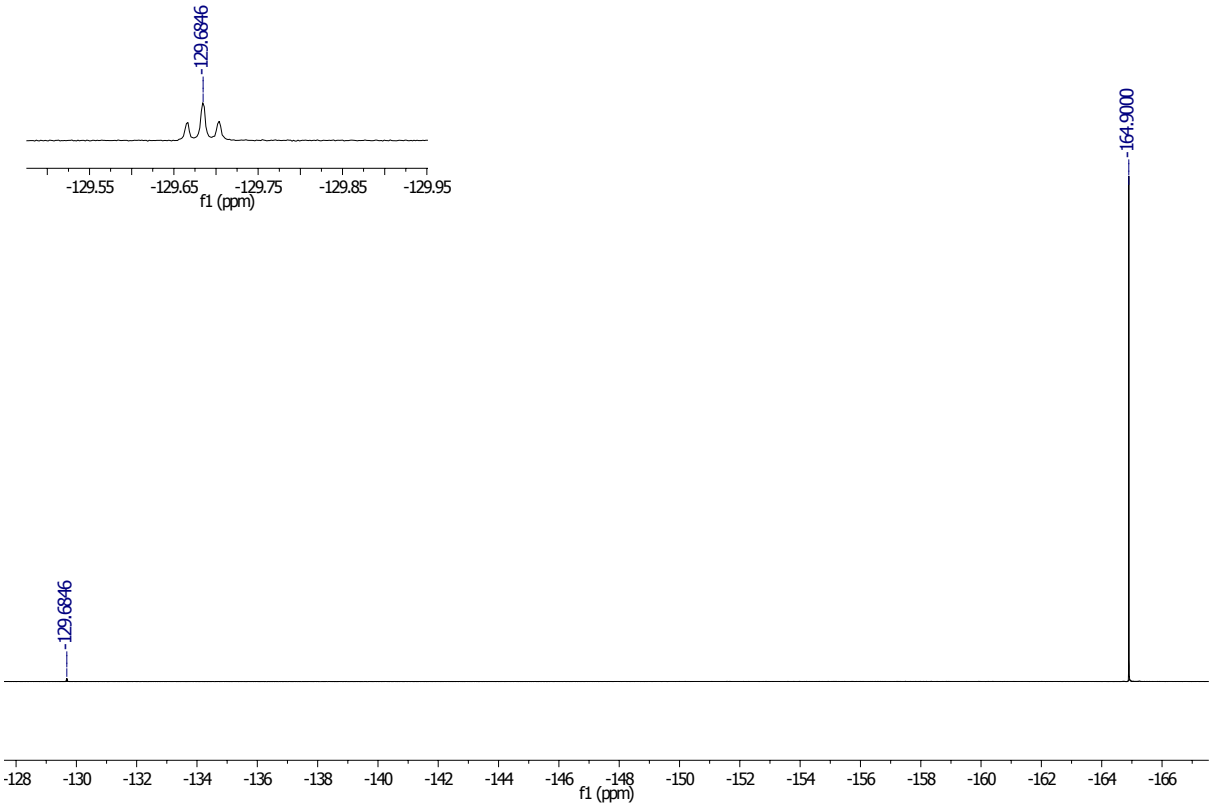

Figure S61. ^{19}F NMR of spectrum of **5** (CD_3CN, 25˚C, 470.6 MHz).

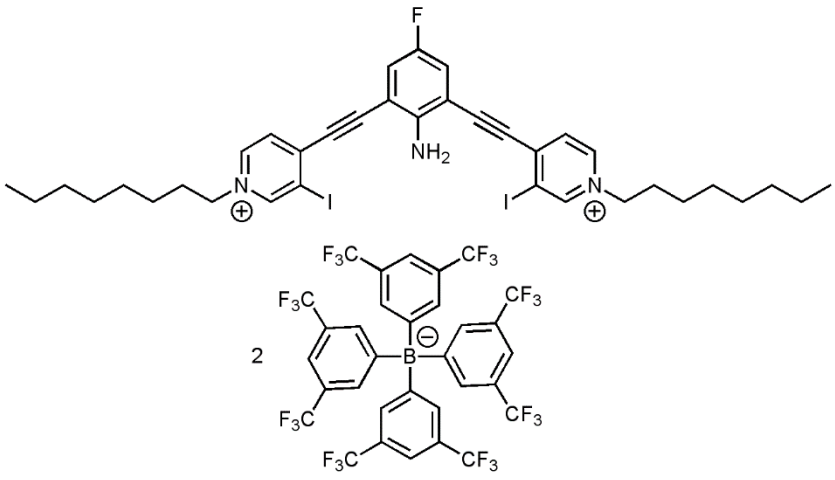

G2XB (6). ^1H (500 MHz, $CDCl_3$, 25˚C): 8.6111 (2H, s), 8.0362-8.0211 (2H, d, *J* = 7.55 Hz), 7.6914 (16H, b), 7.6045-7.5917 (2H, d, *J* = 6.54 Hz), 7.4989 (8H, b), 7.3652-7.3500 (2H, d, *J* = 7.65 Hz), 5.2924 (2H, s), 4.2338 (4H, t, *J* = 7.05 Hz), 1.9174 (4H, b), 1.3144-1.2317 (20H, b), 0.8460 (6H, t). ^{13}C (125.7MHz, $CDCl_3$, 25˚C): 162.2529 (dd, *J*

= 99.95 Hz, *J* = 45.55 Hz), 149.3866, 147.4292, 141.0047, 135.1731, 129.4505 (qq, *J* = 34.07 Hz), 125.9575 (q, *J* = 272.61 Hz), 125.5778, 125.3818, 117.9445, 106.9363, 105.1553 (d, *J* = 7.41 Hz), 99.6546, 95.5300, 63.1093, 31.7955, 31.7420, 29.0824, 28.9629, 26.3058, 22.8052, 14.2414. ^{19}F (470.6 MHz, $CDCl_3$, 25˚C): -126.7810 (1F, t, *J* = 7.65 Hz), -65.3734 (48F, s). HRMS (ESI pos) *m/z*: 395.5805 (M^{+2}, 100%), 1654.2257 (M^{+}-1BAr^{F}); $C_{36}H_{44}FI_2N_3^{+2}$ (395.5814), $C_{68}H_{56}BF_{25}I_2N_3^{+}$ (1654.2241).

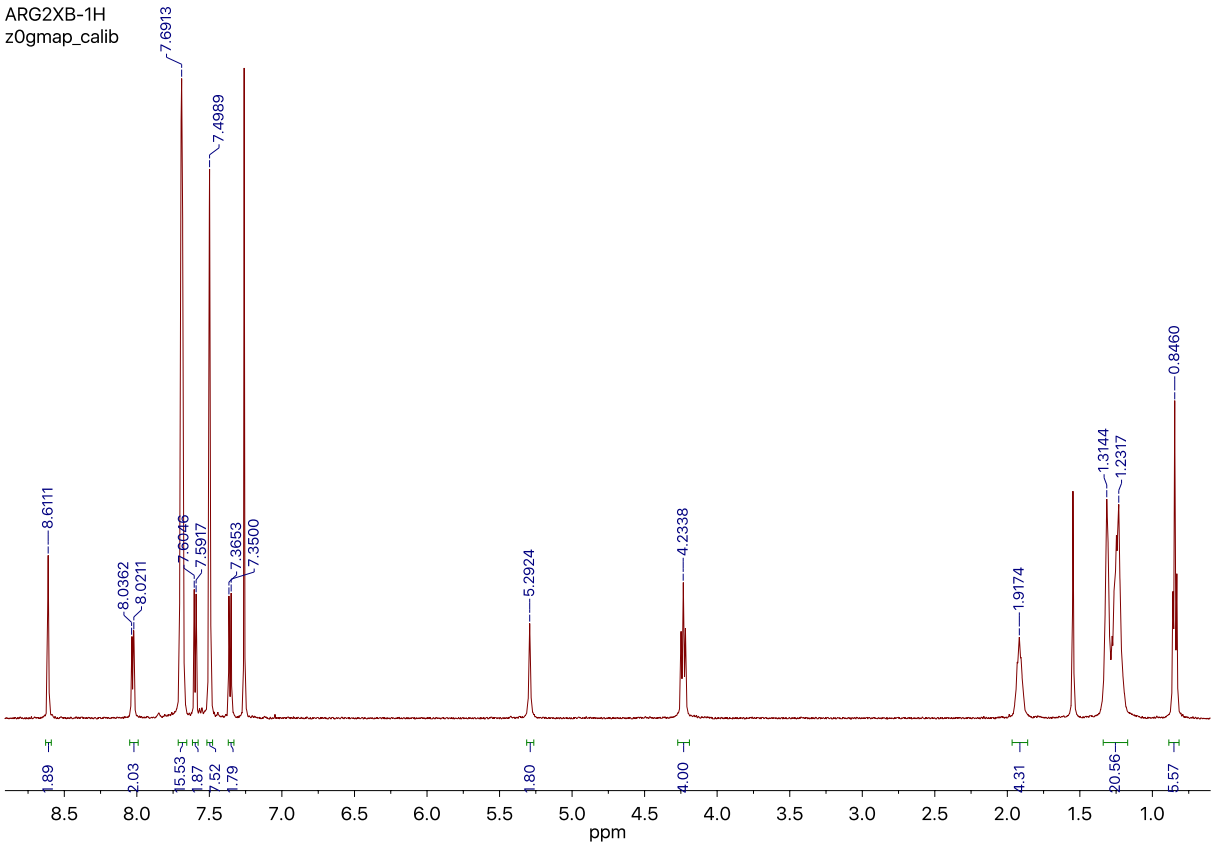

Figure S62. ^{1}H NMR of spectrum of **6** ($CDCl_3$, 25˚C, 500 MHz).

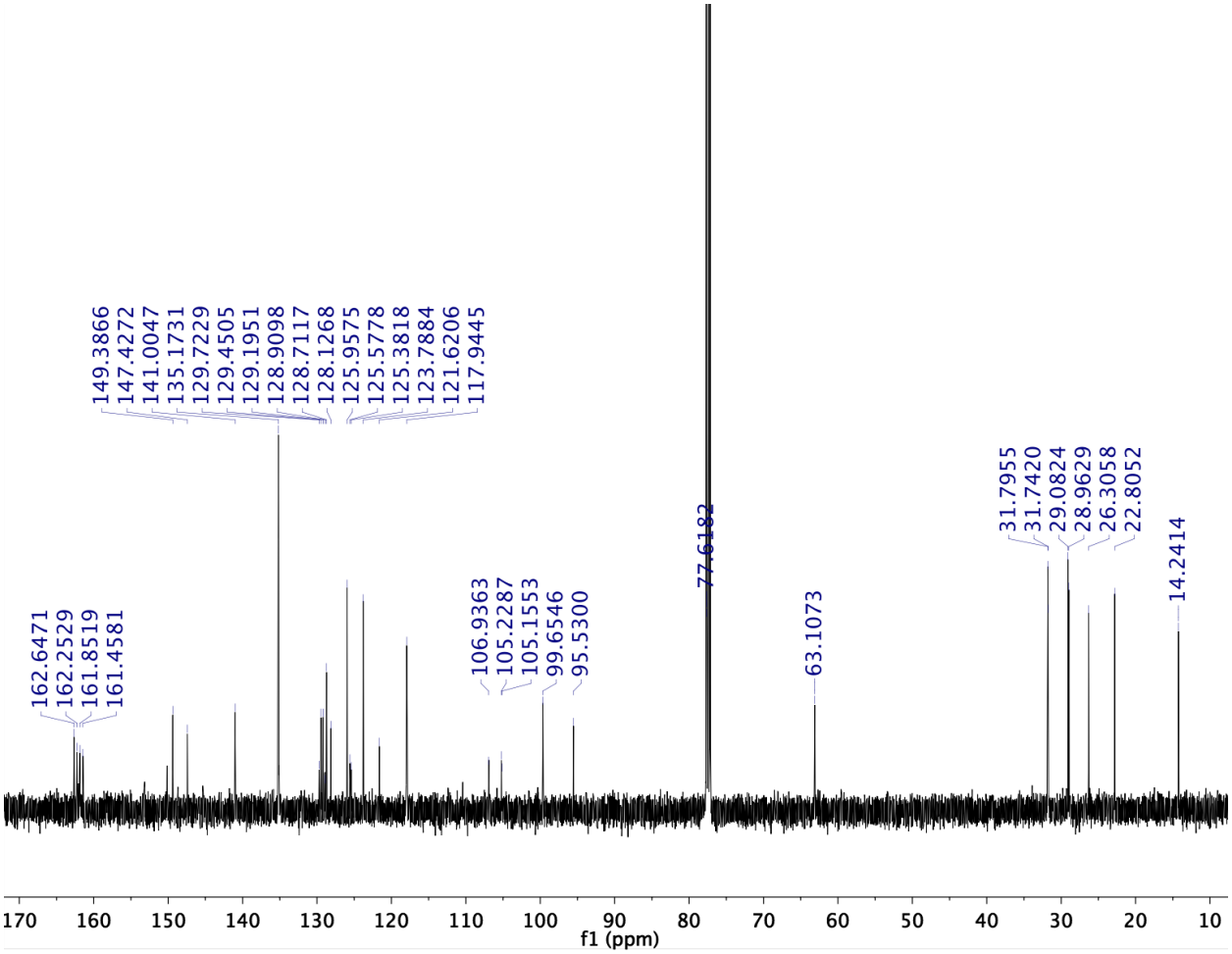

Figure S63. ^{13}C NMR of spectrum of **6** ($CDCl_3$, 25˚C, 125.7 MHz).

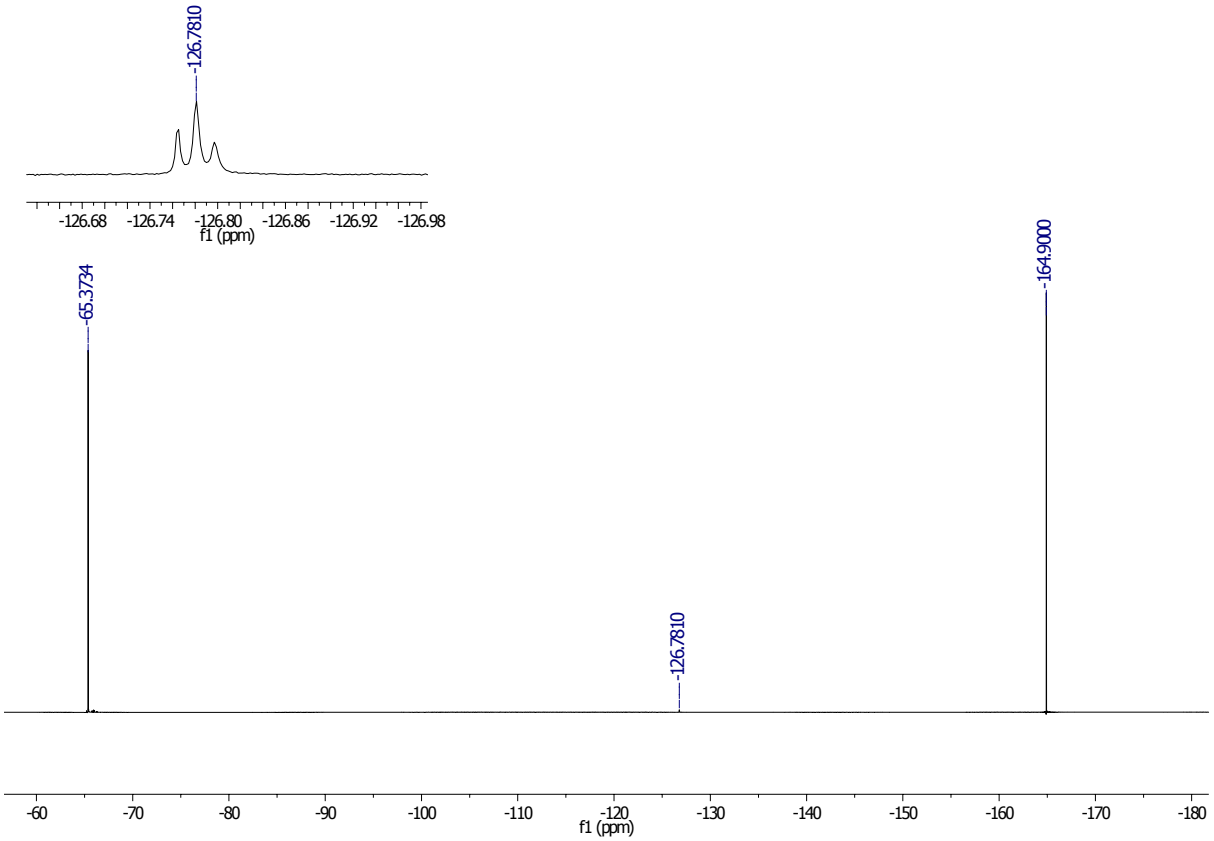

Figure S64. ^{19}F NMR of spectrum of **6** ($CDCl_3$, 25˚C, 470.6 MHz).

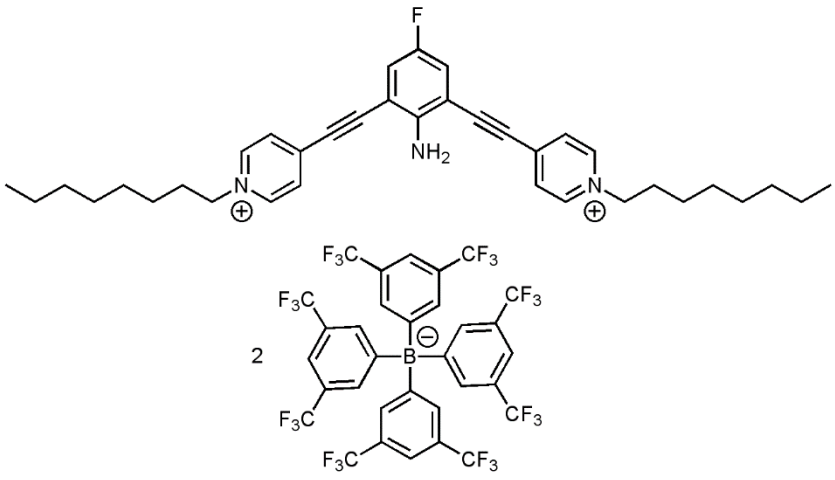

G2HB (7). ^1H (500 MHz, $CDCl_3$, 25˚C): 8.0731-8.0598 (4H, d, *J* = 6.65 Hz), 7.6842 (16H, b), 7.6559-7.6427 (4H, d, *J* = 6.6 Hz), 7.4937 (8H, b), 7.2376 (2H, d), 4.7532 (2H, s), 4.2531 (4H, t, *J* = 7.53 Hz), 1.9058 (4H, b), 1.3076 (20H, b), 0.8548 (6H, t). ^{13}C (125.7 MHz, $CDCl_3$, 25˚C): 161.9838 (dd, *J* = 99.24 Hz, *J* = 49.59 Hz), 148.6799,

142.4386, 141.5833, 134.8523, 129.6429, 129.2233 (qq, *J* = 29.85 Hz), 125.6782 (q, *J* = 272.61 Hz), 124.5287, 124.3342, 117.6843, 117.6541, 105.0244 (d, *J* = 7.55 Hz), 102.6996, 91.0861, 62.9674, 31.5562, 31.4401, 28.8630, 26.0454, 22.5690. ^{19}F (470.6 MHz, $CDCl_3$, 25˚C): -126.9895 (t, *J* = 7.81 Hz, 1F), -65.4280 (48F, s). HRMS (ESI pos) *m/z*: 269.6838 (M^{+2}, 100%), 1402.4325 (M^{+}-1BAr^{F}); $C_{36}H_{44}FI_2N_3^{+2}$ (269.6840), $C_{68}H_{56}BF_{25}I_2N_3^{+}$ (1402.4325).

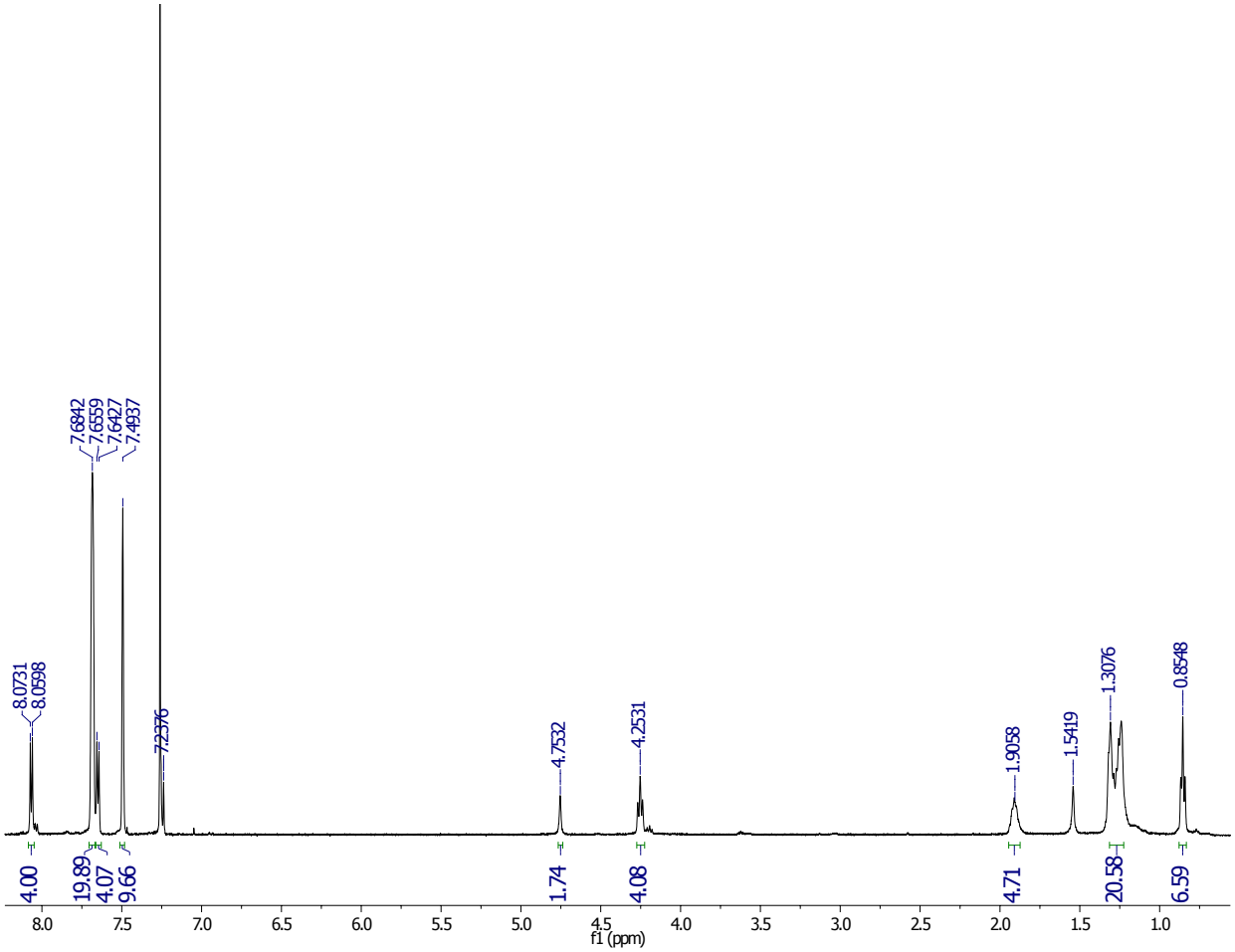

Figure S65. ^{1}H NMR of spectrum of **7** ($CDCl_3$, 25˚C, 500 MHz).

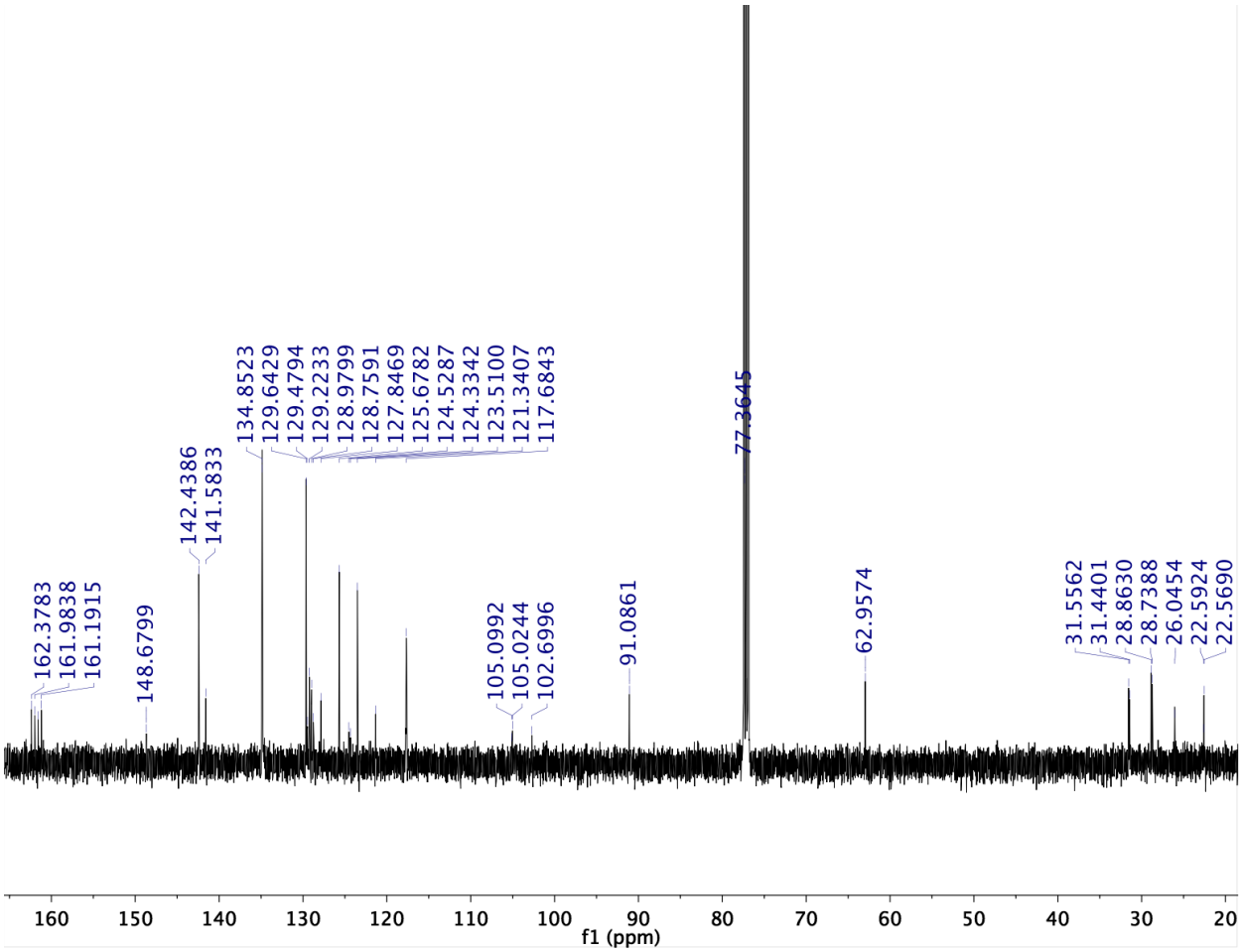

Figure S66. ^{13}C NMR of spectrum of **7** ($CDCl_3$, 25˚C, 125.7 MHz).

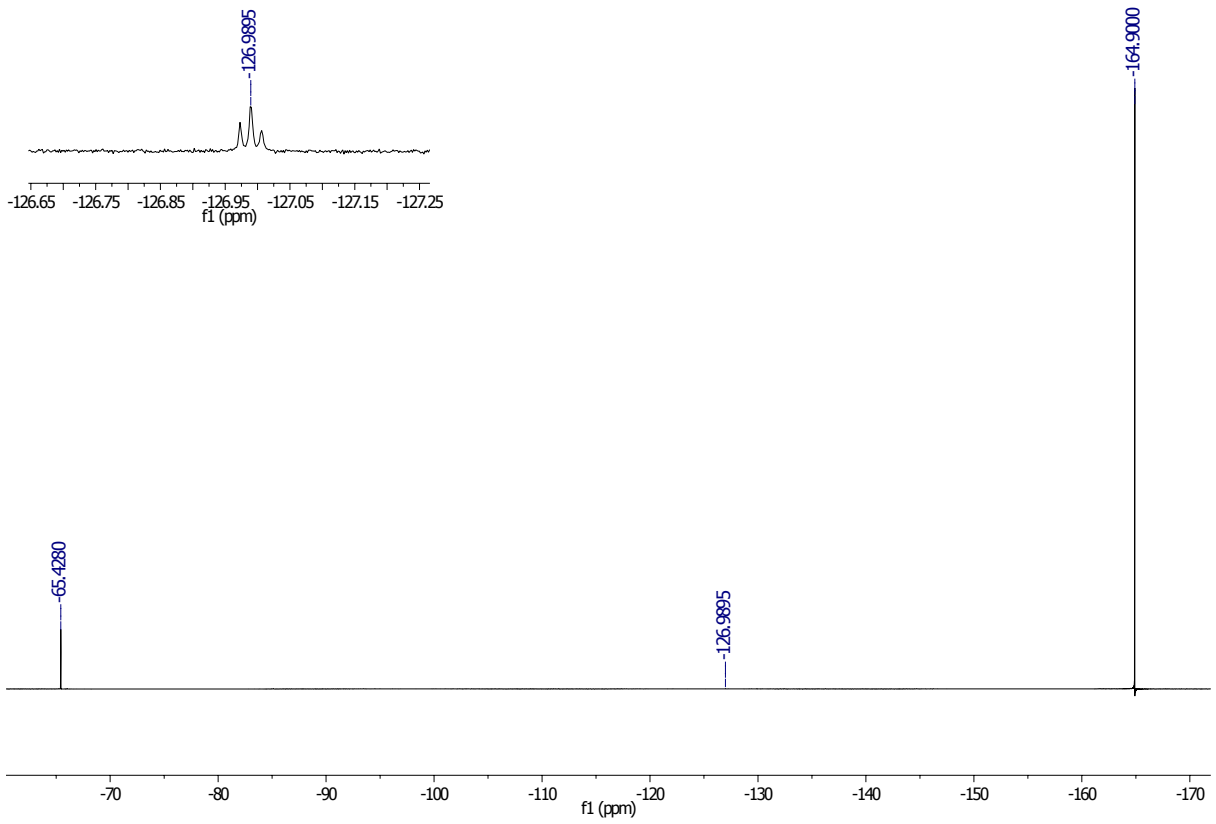

Figure S67. ^{1}H NMR of spectrum of **7** ($CDCl_3$, 25˚C, 470.6 MHz).

G. Computational methods

Computations for **1a**,**b** and **2a**,**b** calculations were carried out with the Gaussian '09 suite of programs using B3LYP functional employing the 6-31+G(d,p) basis set for all atoms except nitrogen and iodine. For which nitrogen—aug-cc-pVTZ basis set and iodide— LANL2DZdp and effective core potential (ECP) were used. The LANL2DZdp ECP basis set was downloaded from the EMSL Basis Set Exchange[3]. To simplify calculations, methyl derivative of charged receptors were evaluated. Crystal structures of methyl derivative of charged XB receptor were employed as a starting point for optimization.

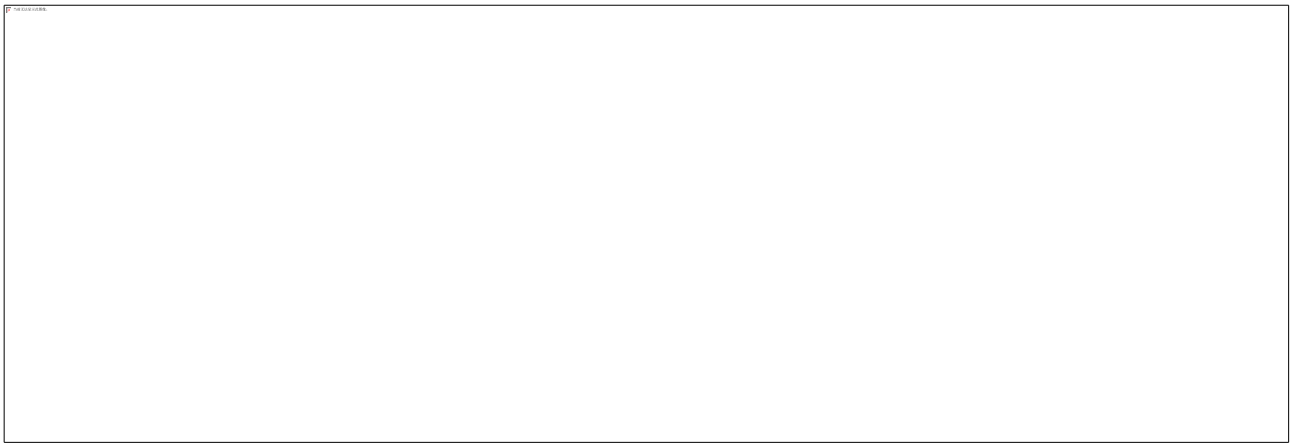

Figure S68. Calculated frontier molecular orbitals for neutral receptors **1a**, **b** and charged receptors **2a**, **b**.

Table 1 Energy of HOMO, LUMO for receptors **1a**, **b** and **2a**, **b.**

	1a	**1b**	**2a**	**2b**
HOMO Energy (eV)	-2.672	-2.506	-8.268	-8.214
LUMO Energy (eV)	-6.011	-6.062	-10.833	-10.844
ΔE (eV)	3.339	3.556	2.565	2.630

Neutral XB receptor **1a**
B3LYP/GEN = -1055.00099255 au

I	3.14731	−2.09014	−0.00006
F	0.	6.0774	0.00037
N	0.	0.55182	0.00003
H	0.86617	0.03944	0.00002
H	−0.86617	0.03944	−0.00002
N	7.23619	−0.71105	0.00009
C	4.72274	0.58018	0.00012
C	4.83728	−0.82734	0.00004
C	3.48258	1.27079	0.00014
C	1.22751	2.63753	0.00018

C	2.45708	1.93045	0.00016
C	6.106	−1.41582	0.00003
H	6.20673	−2.49817	−0.00004
C	0.	1.90735	0.00012
C	−2.45708	1.93045	0.00007
C	1.21173	4.04473	0.00027
H	2.14215	4.60098	0.00032
C	−1.22751	2.63753	0.00014
C	−3.48258	1.27079	0.00001
C	0.	4.71583	0.00029
C	5.93451	1.30647	0.00018
H	5.90825	2.39103	0.00025
C	7.14417	0.62322	0.00016
H	8.08391	1.17093	0.00021
C	−1.21173	4.04473	0.00022
H	−2.14215	4.60098	0.00024
N	−7.23619	−0.71105	−0.00019
C	−4.72274	0.58018	−0.00006
C	−7.14417	0.62322	−0.00011
H	−8.08391	1.17093	−0.0001
C	−5.93451	1.30647	−0.00004
C	−4.83728	−0.82734	−0.00015
C	−6.106	−1.41582	−0.00021
H	−6.20673	−2.49817	−0.00027
I	−3.14731	−2.09014	−0.00018
H	−5.90825	2.39103	0.00002

Neutral HB receptor **1b**

B3LYP/GEN = -1033.43979671 au

F	0.	4.72839	0.0515
N	0.	−0.80336	0.04693
H	−0.85694	−1.279	−0.18102
H	0.85694	−1.279	−0.18102
N	−7.21555	−2.10564	−0.02912
C	−4.74721	−0.7419	−0.0094
C	−4.81019	−2.14535	0.08701
C	−3.50336	−0.04691	−0.00012
C	−1.22643	1.2898	0.02044
C	−2.45977	0.58317	0.00842
C	−6.05776	−2.76591	0.07187
H	−6.12789	−3.84949	0.14559
C	0.	0.56622	0.01783
C	2.45977	0.58317	0.00842
C	−1.21243	2.69739	0.03204
H	−2.14288	3.25337	0.03433
C	1.22643	1.2898	0.02044
C	3.50336	−0.04691	−0.00012

C	0.	3.36725	0.03947
C	-5.96769	-0.04677	-0.11509
H	-5.97981	1.03531	-0.19204
C	-7.15688	-0.77303	-0.11947
H	-8.11059	-0.25507	-0.20026
C	1.21243	2.69739	0.03204
H	2.14289	3.25337	0.03433
N	7.21555	-2.10564	-0.02912
C	4.74721	-0.7419	-0.0094
C	7.15688	-0.77303	-0.11947
H	8.11059	-0.25507	-0.20025
C	5.96769	-0.04677	-0.11509
C	4.81019	-2.14535	0.087
C	6.05776	-2.76591	0.07186
H	6.12789	-3.84949	0.14558
H	5.97981	1.03531	-0.19204
H	3.90357	-2.73497	0.17513
H	-3.90357	-2.73497	0.17514

Charged XB receptor **2a**
B3LYP/GEN = -1134.32828236 au

I	3.5839	-2.10992	-0.00315
F	0.00003	5.95285	-0.00265
N	0.	0.4334	0.00022
H	0.8642	-0.08224	-0.00004
H	-0.86421	-0.08223	-0.00005
N	7.46036	-0.26288	-0.00263
C	4.84095	0.72302	0.00066
C	5.10564	-0.67599	-0.00027
C	3.54736	1.27087	0.00002
C	1.2288	2.52038	-0.00093
C	2.46828	1.84753	-0.00047
C	6.41736	-1.12233	-0.00105
H	6.66683	-2.17589	-0.00153
C	0.00001	1.78238	-0.00059
C	-2.46827	1.84756	-0.0005
C	1.20939	3.93058	-0.0016
H	2.13813	4.48998	-0.00185
C	-1.22879	2.5204	-0.00094
C	-3.54736	1.27093	-0.00006
C	0.00002	4.60678	-0.00197
C	5.96936	1.58514	-0.00005
H	5.82786	2.65927	-0.00135
C	7.24596	1.07644	-0.00118
H	8.12686	1.70708	-0.00217
C	-1.20935	3.93059	-0.00162

H	-2.13808	4.49001	-0.00189
N	-7.46039	-0.26278	-0.00294
C	-4.84096	0.7231	0.00055
C	-7.24598	1.07652	-0.00145
H	-8.12684	1.70721	-0.00252
C	-5.96935	1.58521	-0.00024
C	8.85204	-0.77428	0.02542
H	9.27652	-0.61192	1.01894
H	9.44102	-0.24414	-0.72438
H	8.84678	-1.83882	-0.20391
C	-5.10567	-0.67593	-0.00038
C	-6.41737	-1.12224	-0.00123
H	-6.66688	-2.1758	-0.00171
C	-8.85188	-0.77463	0.0263
H	-9.27169	-0.62311	1.02355
H	-8.84765	-1.83659	-0.21479
H	-9.44443	-0.23644	-0.71483
I	-3.58393	-2.10985	-0.00325
H	-5.82786	2.65934	-0.00162

Charged HB receptor **2b**

B3LYP/GEN = -1112.77851060 au

H	4.31962	-1.41665	-0.00176
F	0.00003	5.95285	-0.00265
N	0.	0.4334	0.00022
H	0.8642	-0.08224	-0.00004
H	-0.86421	-0.08223	-0.00005
N	7.46036	-0.26288	-0.00263
C	4.84095	0.72302	0.00066
C	5.10564	-0.67599	-0.00027
C	3.54736	1.27087	0.00002
C	1.2288	2.52038	-0.00093
C	2.46828	1.84753	-0.00047
C	6.41736	-1.12233	-0.00105
H	6.66683	-2.17589	-0.00153
C	0.00001	1.78238	-0.00059
C	-2.46827	1.84756	-0.0005
C	1.20939	3.93058	-0.0016
H	2.13813	4.48998	-0.00185
C	-1.22879	2.5204	-0.00094
C	-3.54736	1.27093	-0.00006
C	0.00002	4.60678	-0.00197
C	5.96936	1.58514	-0.00005
H	5.82786	2.65927	-0.00135
C	7.24596	1.07644	-0.00118
H	8.12686	1.70708	-0.00217

C	-1.20935	3.93059	-0.00162
H	-2.13808	4.49001	-0.00189
N	-7.46039	-0.26278	-0.00294
C	-4.84096	0.7231	0.00055
C	-7.24598	1.07652	-0.00145
H	-8.12684	1.70721	-0.00252
C	-5.96935	1.58521	-0.00024
C	8.85204	-0.77428	0.02542
H	9.27652	-0.61192	1.01894
H	9.44102	-0.24414	-0.72438
H	8.84678	-1.83882	-0.20391
C	-5.10567	-0.67593	-0.00038
C	-6.41737	-1.12224	-0.00123
H	-6.66688	-2.1758	-0.00171
C	-8.85188	-0.77463	0.0263
H	-9.27169	-0.62311	1.02355
H	-8.84765	-1.83659	-0.21479
H	-9.44443	-0.23644	-0.71483
H	-4.31965	-1.41659	-0.00186
H	-5.82786	2.65934	-0.00162

H. Reference

1. Kamlet, M. J., Abboud, J. L., & Taft, R. W. (1977). *Journal of the American Chemical Society*, 99(18), 6027-6038.

2. Reichardt, C. (1994). *Chemical Reviews*, *94*(8), 2319-2358.

3. https://bse.pnl.gov/bse/portal